**THE EUROPEAN
PHYSICAL JOURNAL B**

Composite spin-triplet superconductivity in an $SU(2) \otimes SU(2)$ symmetric lattice model

F.B. Anders[a]

Institut für Festkörperphysik, Technical University Darmstadt, 64289 Darmstadt, Germany

Abstract. The two-channel Anderson lattice model which has $SU(2) \otimes SU(2)$ symmetry is of relevance to understanding of the magnetic, quadrupolar and superconducting phases in $U_{1-x}Th_xBe_{13}$ or Pr based skutterudite compounds such as $PrFe_4P_{12}$ or $PrOs_4Sb_{12}$. Possible unconventional superconducting phases of the model are explored. They are characterized by a composite order parameter comprising of a local magnetic or quadrupolar moment and a triplet conduction electron Cooper-pair. This binding of local degrees of freedom removes the entropy of the non Fermi-liquid normal state. We find superconducting transitions in the intermediate valence regime which are suppressed in the stable moment regime. The gap function is non analytic and odd in frequency: a pseudo-gap develops in the conduction electron density of states which vanishes as $|\omega|$ close to $\omega = 0$. In the strong intermediate valent regime, the gap function acquires an additional $\boldsymbol{k}$-dependence.

PACS. 74.20.-z Theories and models of superconducting state – 74.20.Mn Nonconventional mechanisms – 75.10.Lp Band and itinerant models – 75.30.Mb Valence fluctuation, Kondo lattice, and heavy-fermion phenomena

1 Introduction

Superconductivity or superfluidity of ^{3}He [1] is understood to be a thermodynamic phase in which spin 1/2 Fermions are subject to Cooper-pair correlations and condense. The Fermions are either electrons or ^{3}He atoms. Superconductivity is well described by the Bardeen-Cooper-Schrieffer (BCS) theory [2] when the fluctuations of the order parameter are small. The Eliashberg theory of superconductivity [3,4] is applicable in superconductors when high and low energy scales are well separated. Contrary to the BCS theory, this theory accounts for the retardation of the interaction mediating bosons. On a large time scale, the electron repulsion is effectively overcome in standard superconductors by the electron-phonon interaction. The small parameter needed for the applicability of the Eliashberg theory is given by the ratio of the Debye frequency and the Fermi energy. It is well known that Eliashberg theory cannot be used in the ^{3}He problem [1] since no separation of energy scales can be found here. ^{3}He atoms pair in spin triplets and orbital momentum of $L = 1$ in contrast to standard superconductors which usually develop spin singlets pairing. The rich phase diagram of ^{3}He is directly related to this anisotropic pair-condensation. Pairs with $L = 1$ have nodes in space and, therefore, can effectively overcome the hard-core repulsion and gain condensation energy.

Heavy fermion materials [5] have drawn much attention since the discovery of superconductivity in $CeCu_2Si_2$ [6], which seems to be characterized by an anisotropic order parameter with a symmetry yet to be determined. Another example for an anisotropic order parameter are the high temperature cuprate superconductors. Their current carrying subsystem consists of layered copper oxide perovskite structures. Strong experimental evidence has been compiled for an unconventional order parameter in these materials, with Γ_2 symmetry of the form $\cos(k_x a) - \cos(k_y a)$ or $(k_x^2 - k_y^2)$ which is usually called "d-wave" superconductivity by many authors. A superconductor is called *conventional* if the order parameter has the full symmetry of the Fermi-surface; the order parameter still might be anisotropic but it transforms in accordance with the trivial irreducible representation of the point-group Γ_1. Otherwise, the order parameter is called *unconventional*. Recently, the superconductivity of Sr_2RuO_4 has generated strong interest due to structural similarities between this compound and the *High-T_c* materials [7]. It has been suggested that Sr_2RuO_4 might be an example of an unconventional spin triplet superconductor [8,9] in contrast to the *High-T_c* materials where a Γ_2 symmetry is favoured. In spite of the progress in our understanding of Heavy Fermion materials, there has been little success in determining the symmetry of their order parameters in the superconducting phase. Huth *et al.* recently reported experimental evidence which indicates an

[a] e-mail: frithjof@fkp.tu-darmstadt.de

electronically mediated pair-condensation mechanism in UPd$_2$Al$_3$ [10]. Our theoretical understanding of unconventional superconductivity is still far from complete in spite of more than 20 years of research. Theories were developed along two basic lines: either the superconducting phase of microscopic models was investigated using, at that time, state of the art approximations in order to reveal possible pairing mechanisms, or phenomenological approaches, based on the Ginsburg-Landau theory, were constructed in order to give new insight into the possible symmetries of the order parameter and their impact on the measurable quantities [11].

Two channel Anderson and Kondo lattice models exhibit non-Fermi liquid behaviour in the paramagnetic phase driven by unquenched and fluctuating local degrees of freedom [12,13]. This phase is characterized by a large residual resistivity and entropy, and ill defined electronic quasi-particles. Fermi liquid physics is restored by cooperative ordering or applied magnetic field or stress [13,14]. In particular, for a non Kramer's doublet crystal field state in U^{4+} or Pr^{3+} ions, a two channel Kondo effect is possible [15]. The magnetic "spin" of the electrons serves as channel index in this case. UBe$_{13}$ and PrFeP$_{12}$ are prominent candidates for a quadrupolar Kondo lattice description, as their enormous resistivity ($> 100~\mu\Omega$cm) is removed only by phase transitions (superconductivity in UBe$_{13}$, antiferroquadrupolar order in PrFeP$_{12}$). Indeed, it has been shown that commensurate and incommensurate orbital ordering, as well as ferromagnetism are possible in this model depending upon coupling strength and filling [14]. Evidence of a first order transition to an odd frequency pairing state in the Kondo limit (near integral valence) has been adduced, which is a singlet in both spin and channel indices, and no $\boldsymbol{q}$ value was preferred for the center of mass momentum [13].

Our paper is organized as follows. In Section 2, we review the two-channel Anderson lattice model [12]. This model is rotational invariant in spin and channel space and, therefore, has $SU(2) \otimes SU(2)$ symmetry. We use established standard methods developed by others [12–14,16–22] to obtain an approximate solution of its one- and two-particle properties. In Section 3, all possible spin and channel symmetry sectors of Cooper-pairs are discussed. Two of the four sectors require odd-frequency gap functions [23] if we restrict ourselves to $\boldsymbol{k}$-dependence with Γ_1 symmetry. We discuss the concept of a composite order parameter in Section 3.3. A connection between the composite order parameter and the Cooper-pair susceptibility is made in Section 3.4. The statements of Section 3 are exact and independent of any approximation. The solution of the homogeneous phase of the model [12] is used to obtain the superconducting transition temperature defined by the divergence of the pair-susceptibility which will be the subject of Section 4. In Section 5, we present the self-consistency equations for the triplet/triplet 8×8 Nambu matrix Green function, which is the so-called *dynamical mean field theory* (DMFT) [24,21,22] analog of the Eliashberg equation. However, no Migdal theorem is required since the full local irreducible pairing vertex is used. This non-perturbative set of equations lead to quasiparticle and anomalous Green functions which are gapped at $\omega = 0$, as shown in Section 5.4. The gap function is nonanalytic in frequency, and, therefore, Heid's theorem [25] is not applicable. This superconducting phase belongs to a minimum of the free energy.

2 Theory

2.1 Model

Uranium based Heavy Fermion materials exhibit a lot of interesting and unusual physical properties: coexistence of magnetism with superconductivity and non-Fermi liquid behaviour in the paramagnetic phase. The uranium $5f$-shell states in Heavy Fermion compounds can be $5f^1$ (U^{5+}), $5f^2$ (U^{4+}) and $5f^3$ (U^{3+}). Experimentally, however, U^{5+} is energetically unlikely. The Hund's rules ground state multiplets are given by $J = 5/2$, $J = 4$ and $J = 9/2$ respectively and split in a cubic symmetry [26] according to the irreducible representationss of the point group. If we consider only valence fluctuations between the lowest irreducible representationss of $5f^2 \leftrightarrow 5f^3$ or $5f^2 \leftrightarrow 5f^1$, the uranium $5f$-shell is modelled by a magnetic doublet $\Gamma_6(\Gamma_7)$ above a non-Kramers Γ_3 doublet ground state which has a quadrupolar, and hence orbital character. Only conduction electrons with Γ_8 symmetry, labelled by a spin σ and a locally defined orbital index α, couple to these ionic states according to a simple group-theoretical selection rule [15,27]. The same arguments also apply to Pr^{3+} ($J = 4$) and Pr^{4+} ($J = 5/2$) in a cubic crystalline environment which is found in the skutterudite materials PrFe$_4$P$_{12}$, which shows anitferro-quadrupolar order around 2K, and PrOs$_4$Sb$_{12}$ where a superconducting transition was found at $2K$ [28]. If we restrict ourselves to local hybridization and coupling to two generate band – an assumption which we will justify within the DMFT the lattice model on a cubic lattice

$$
\begin{aligned}
H = &\sum_{\boldsymbol{k}\sigma\alpha} \varepsilon_{\boldsymbol{k}\sigma\alpha} c_{\boldsymbol{k}\alpha\sigma}^{\dagger} c_{\boldsymbol{k}\alpha\sigma} + \sum_{\sigma\nu} E_{\sigma} X_{\Gamma_6\sigma,\Gamma_6\sigma}^{\nu} \\
&+ \sum_{\alpha\nu} E_{\alpha} X_{\Gamma_3\alpha,\Gamma_3\alpha}^{\nu} + \frac{1}{\sqrt{N}} \sum_{\nu\alpha\sigma} \left(V_{\alpha} c_{\nu\alpha\sigma}^{\dagger} X_{\Gamma_3-\alpha,\Gamma_6\sigma}^{\nu} + \text{h.c.} \right)
\end{aligned}
\tag{1}
$$

has an $SU(2) \otimes SU(2)$ symmetric with respect the spin σ and channel α space. $X_{\gamma,\gamma'}^{\nu}$ are the usual Hubbard projection operators [29] at lattice site ν which describe transitions from local $4(5)f$ atomic state γ' to the state γ.

The Hamiltonian (1) contains three different energy scales: the band-width D of the conduction bands $\varepsilon_{\alpha\sigma}$, the inter-configurational energy $\varepsilon_{\alpha\sigma} = E_{\sigma} - E_{\alpha}$ and the so-called Anderson or hybridization width $\Delta \equiv \pi\rho_0 V^2$, ρ_0 is the conduction electron density of states at the chemical potential $\mu = 0$. If not otherwise stated, we will use Δ as the energy-scale throughout this paper.

2.2 Dynamical mean field theory

The fundamental assumption of the DMFT is the locality of single particle self-energy which allows the mapping of a complicated lattice problem onto an effective site problem [16,30] which is embedded in a fictitious bath of conduction electrons. This bath, the so-called media, takes into account the angular averaged but energy dependent influence of the lattice onto this effective site. The DMFT self-consistency condition (SCC) demands the equality of the $\boldsymbol{k}$-summed lattice Green function with the Green function of the effective site. Then, only one-particle irreducible loops, which describe the hopping of a single electron from and to the effective site, enters the SCC. Any two particle irreducible loops – correlated hopping of two electrons from and back onto the site – are factorized in a product of one-particle loops: higher order correlations which also contribute to a local self-energy, are neglected. This assumption becomes exact in the limit of infinity spatial dimensions [18,21,22].

Even if we had taken into account a band dispersion $\varepsilon_{\boldsymbol{k}\sigma\alpha\alpha'}$, non-diagonal in the orbital index α, the mapping onto an effective site requires two locally defined, degenerate effective conduction bands which are symmetry projected linear combinations of the Wannier state of the conduction bands. Cox has shown that only those hybridize with the local f-states on symmetry grounds [15]. Since the local dynamics is governed by the correlations induced by the f-states, it is consistent with the DMFT to restrict ourselves to diagonal band dispersions $\varepsilon_{\boldsymbol{k}\sigma\alpha}$ in equation (1). We use the so-called Non-Crossing Approximation (NCA) [31–33] as a solver for the effective impurity throughout the paper since it has been established as standard technique for solving the two-channel lattice model [12,14].

2.2.1 Single-particle green function

The conduction electron Green function $G_{\alpha\sigma}(\boldsymbol{k}, z)$ for the model (1) obeys the exact equation of motion:

$$G_{\alpha\sigma}(\boldsymbol{k}, z) = \frac{1}{z - \varepsilon_{\boldsymbol{k}\alpha\sigma}} + \frac{1}{z - \varepsilon_{\boldsymbol{k}\alpha\sigma}} |V_\alpha|^2 F_{\alpha\sigma}(\boldsymbol{k}, z) \frac{1}{z - \varepsilon_{\boldsymbol{k}\alpha\sigma}}, \quad (2)$$

which connects it to the f-Green function

$$F_{\alpha\sigma}(\boldsymbol{k}, z) = \frac{1}{N} \sum_i e^{i\boldsymbol{k}\boldsymbol{R}_i} \left\langle\left\langle X^i_{-\alpha,\sigma} | X^i_{\sigma,-\alpha} \right\rangle\right\rangle(z). \quad (3)$$

Since $F_{\alpha\sigma}(\boldsymbol{k}, z)$ can always be written as

$$F_{\alpha\sigma}(\boldsymbol{k}, z) = \left[\bar{F}^{-1}_{\alpha\sigma}(\boldsymbol{k}, z) - \frac{|V_\alpha|^2}{z - \varepsilon_{\boldsymbol{k}\alpha\sigma}} \right]^{-1}, \quad (4)$$

where in DMFT $\bar{F}^{-1}_{\alpha\sigma}(\boldsymbol{k}, z) = \bar{F}^{-1}_{\alpha\sigma}(z) = z - \varepsilon_{\alpha\sigma} - \Sigma^f_{\alpha\sigma}(z)$, the DMFT solution for the single-particle Green function

of two-channel periodic Anderson model is determined by the solution of

$$\begin{aligned} F_{loc,\alpha\sigma}(z) &= \frac{1}{z - \varepsilon_{\alpha\sigma} - \Delta_{\alpha\sigma}(z) - \Sigma^f_{\alpha\sigma}(z)} \\ &= \frac{1}{N} \sum_{\boldsymbol{k}} \left[\bar{F}^{-1}_{\alpha\sigma}(z) - \frac{|V_\alpha|^2}{z - \varepsilon_{\boldsymbol{k}\alpha\sigma}} \right]^{-1}. \end{aligned} \quad (5)$$

The local self-energy $\Sigma^f_{\alpha\sigma}(z)$ is calculated by a SIAM with an effective conduction-electron density of states $\tilde{\rho}(\omega) = \Im m \Delta(\omega - i\delta)/|\pi V_\alpha^2|$. Therefore, the self-energy of the conduction electrons $\Sigma^c_{\alpha\sigma}(\boldsymbol{k}, z) = z - \varepsilon_{\boldsymbol{k}\alpha\sigma} - G^{-1}_{\alpha\sigma}(\boldsymbol{k}, z)$ is given by

$$\Sigma^{(c)}_{\alpha\sigma}(z) = \frac{T_{\alpha\sigma}(z)}{1 + \tilde{G}T_{\alpha\sigma}(z)} = \frac{|V_\alpha|^2}{z - \varepsilon_{\alpha\sigma} - \Sigma^f_{\alpha\sigma}(z)} \quad (6)$$

as a consequence of the equation of motion (2) where $T_{\alpha\sigma}(z) = |V_\alpha|^2 \bar{F}_{\alpha\sigma}(z)$. Equations (2–6) are valid for any number of channels.

In contrast to the single channel Kondo effect, the ground state cannot be mapped onto a renormalized Fermi liquid in the two channel case. Here, the effective coupling constant flows to an intermediate value. The corresponding fixed point has non-Fermi liquid properties and is unstable against a magnetic and a channel field [34].

The single particle and transport properties of this model [12] show non-Fermi liquid-behaviour within the DMFT approximation which can be seen immediately by the analytic form of the conduction electron self-energy (6): independent on the method which is used to solve the effective impurity, the local f-self-energy $\Sigma^f_{\alpha\sigma}(z)$ and, therefore, also self-energy of the conduction electrons, must have a finite imaginary part even for $T \to 0$ in the paramagnetic phase since the local T-matrix is pinned to half of the unitary limit [27,34,35]. The scattering originates in the two-channel Kondo effect in the impurity model [15]: the local quadrupolar moments of the Γ_3 states are dynamically screened by the conduction electrons orbital moments, if $E_\alpha < E_\sigma$. In the case of $E_\alpha > E_\sigma$, orbital and spin degrees of freedom are interchanged, and the local magnetic moments are screened instead. The predicted excitation gap at low temperatures in the optical conductivity [12] has been found in UBe$_{13}$ [36].

This result of a finite resistivity in the paramagnetic phase, originating in magnetic scattering at the f-sites due to the absents of singlet ground state, indicates the instability of this phase towards those phase transitions which will remove the residual entropy of the lattice. We showed in a previous publication [14], that the model has a rich phase diagram of spin-density, quadrupolar-density, and anti-ferromagnetic and anti-quadrupolar order for larger $|\varepsilon_{\alpha\sigma}| > \Delta$. For the intermediate valent regime ($|\varepsilon_{\alpha\sigma}| < \Delta$) ferromagnetism is found for small band fillings. We suspect, that superconductivity dominates the intermediate valent regime.
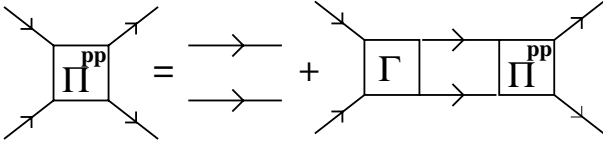
Fig. 1. Bethe-Salpeter equation for the two-particle Green function Π^{pp}, Γ denotes the irreducible vertex.

2.2.2 Particle-particle green function

The main focus of this investigation is devoted to the study of superconducting transitions. One indicator of a phase transition is a divergence of the static order parameter susceptibility. Therefore, we are interested in Fourier components of space-time susceptibilities of the type

$$\chi_{O_i,O_j}(t) = -\left\langle T(O_i(t)\, O_j^\dagger) \right\rangle, \tag{7}$$

where O_i will be a symmetry adapted Cooper pair operator $c_{i\alpha\sigma}c_{i\alpha'\sigma'}$. The lattice susceptibilities are obtained as

$$\chi_O(\boldsymbol{q},\nu) = \frac{1}{N^2\beta^2} \sum_{\mathrm{i}\omega_n,\boldsymbol{k},\mathrm{i}\omega_m\boldsymbol{k}'} F_O(\mathrm{i}\omega_n,\boldsymbol{k})F_O^*(\mathrm{i}\omega_m,\boldsymbol{k}')$$
$$\times \Pi(\mathrm{i}\omega_n,\boldsymbol{k};\mathrm{i}\omega_m,\boldsymbol{k}')(\boldsymbol{q},\nu), \tag{8}$$

where $F_O(\mathrm{i}\omega_n,\boldsymbol{k})$ is the Fourier component of the structure factor of the operator $O_i(t)$ and $\Pi(\mathrm{i}\omega_n,\boldsymbol{k};\mathrm{i}\omega_m,\boldsymbol{k}')(\boldsymbol{q},\nu)$ denotes the two-particle Green function. The summation over spin and channel indices has been omitted in the following section for clarity. It will be introduced and discussed in Section 3.4.

The two-particle Green function Π obeys a Bethe-Salpeter equation, diagrammatically depicted in Figure 1. The lines are fully renormalized one-particle Green functions. A scaling analysis has proven that the total irreducible vertex has to be purely local in the limit of infinite spatial dimensions [37,38]. Total irreducibility means that each diagrammatic part remains connected when any two electron lines are cut. Although, we use the textbook definition of two-particle irreducibility with respect to Feynman perturbation theory, the structure of the equations are invariant of the underlying perturbation theory since the Bethe-Salpeter equation is the two-particle equivalent to the Dyson equation.

It was noticed early in the development of the DMFT [24,38] that only the local part of the irreducible two-particle vertex enters the Bethe-Salpeter equation for the two-particle Green function. Moreover, the renormalization of the one-particle self-energy by the two-particle vertex is already taken into account in DMFT [21,22]. This statement, however, is only true inside the homogeneous (paramagnetic) phase. The susceptibility becomes divergent near the phase transition temperature T_c where at least one irreducible vertex diverges and becomes $\boldsymbol{k}$-dependent. The scaling argument fails in this case. Therefore, the self-energy Σ acquires an additional, possible $\boldsymbol{k}$-dependent, contribution in the symmetry broken phase.

This has been widely used to investigate possible magnetic and superconduction phases in various models [13,20,39].

With a local irreducible pp-vertex Γ in the homogeneous phase, the particle-particle Green function Π reads

$$\Pi(\mathrm{i}\omega_n,\boldsymbol{k};\mathrm{i}\omega_m,\boldsymbol{k}')(\boldsymbol{q},\mathrm{i}\nu_n) =$$
$$\beta N\delta_{\boldsymbol{k},\boldsymbol{k}'}\delta_{n,m}\Pi_{free}(\boldsymbol{k},\boldsymbol{q},\mathrm{i}\omega_n,\mathrm{i}\nu_n) \tag{9}$$
$$+\Pi_{free}(\boldsymbol{k},\boldsymbol{q},\mathrm{i}\omega_n,\mathrm{i}\nu_n)I(\mathrm{i}\omega_n,\mathrm{i}\omega_m,\mathrm{i}\nu_n,\boldsymbol{q})$$
$$\times \Pi_{free}(\boldsymbol{k}',\boldsymbol{q},\mathrm{i}\omega_m,\mathrm{i}\nu_n), \tag{10}$$

where

$$\Pi_{free}(\boldsymbol{k},\boldsymbol{q},\mathrm{i}\omega_n,\mathrm{i}\nu_n) = G_{\boldsymbol{k}+\boldsymbol{q}}(\mathrm{i}\omega_n+\mathrm{i}\nu_n)G_{-\boldsymbol{k}}(\mathrm{i}\omega_n) \tag{11}$$

and the reducible vertex $I(\mathrm{i}\omega_n,\mathrm{i}\omega_m,\mathrm{i}\nu_n,\boldsymbol{q})$ obeys the Bethe-Salpeter equation

$$I(\mathrm{i}\omega_n,\mathrm{i}\omega_m,\mathrm{i}\nu_n,\boldsymbol{q}) = \Gamma(\mathrm{i}\omega_n,\mathrm{i}\omega_m;\mathrm{i}\nu_n)$$
$$+\frac{1}{\beta}\sum_{i\omega_{n'}}\Gamma(\mathrm{i}\omega_n,i\omega_{n'};\mathrm{i}\nu_n)$$
$$\times \chi_0(iw_{n'};\mathrm{i}\nu_n,\boldsymbol{q})I(i\omega_{n'},\mathrm{i}\omega_m)(\mathrm{i}\nu_n,\boldsymbol{q}). \tag{12}$$

Herein, the particle-particle bubble $\chi_0(i\omega_n;\mathrm{i}\nu_n,\boldsymbol{q})$ is given by

$$\chi_0(i\omega_n;\mathrm{i}\nu_n,\boldsymbol{q}) = \frac{1}{N}\sum_{\boldsymbol{k}}\Pi_{free}(\boldsymbol{k},\boldsymbol{q},\mathrm{i}\omega_n,\mathrm{i}\nu_n). \tag{13}$$

Energy $\mathrm{i}\nu_n$ and momentum $\boldsymbol{q}$ of the center of mass (COM) are conserved. It was shown [24] that the COM-momentum only enters through a scalar $\eta(\boldsymbol{q})$

$$\eta(\boldsymbol{q}) = \frac{1}{d}\sum_{\alpha}^{d}\cos(q_\alpha) \tag{14}$$

on a hyper-cubic lattice in d dimensions. In this case, equation (12) is casted into a matrix equation in Matsubara-frequency space

$$\underline{\underline{I}}(\mathrm{i}\nu_n,\boldsymbol{q}) = \underline{\underline{\Gamma}}(\mathrm{i}\nu_n) + \frac{1}{\beta}\underline{\underline{\Gamma}}(\mathrm{i}\nu_n)\underline{\underline{\chi}}_0(\mathrm{i}\nu_n,\boldsymbol{q})\underline{\underline{I}}(\mathrm{i}\nu_n,\boldsymbol{q}), \tag{15}$$

which is formally solved by

$$\underline{\underline{I}}(\mathrm{i}\nu_n,\boldsymbol{q}) = \left[1 - \frac{1}{\beta}\underline{\underline{\Gamma}}(\mathrm{i}\nu_n)\underline{\underline{\chi}}_0(\mathrm{i}\nu_n,\boldsymbol{q})\right]^{-1}\underline{\underline{\Gamma}}(\mathrm{i}\nu_n). \tag{16}$$

The DMFT mapping of the lattice problem onto an effective impurity problem is used in order to calculate the irreducible vertex $\underline{\underline{\Gamma}}^{ph}(\mathrm{i}\nu_n)$. In formal equivalence to equation (15), the equation

$$\underline{\underline{\Pi}}_{loc}(\mathrm{i}\nu_n) = \beta\underline{\underline{\chi}}_{loc} + \underline{\underline{\chi}}_{loc}\frac{1}{\beta}\underline{\underline{\Gamma}}(\mathrm{i}\nu_n)\underline{\underline{\Pi}}_{loc}(\mathrm{i}\nu_n), \tag{17}$$

depicted in Figure 1, holds for the local two-particle Green function of the effective site. It has been shown that the
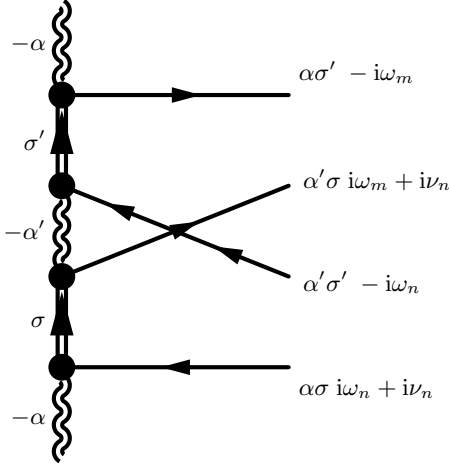
Fig. 2. Local particle-particle Green function for the two-channel model in NCA plotted on an imaginary time axis, from bottom to top. The wiggly vertical line represents the Γ_3 states, the double straight the magnetic Γ_6 states and the horizonal lines the hybridizating conduction electrons.

irreducible vertices $\underline{\underline{\Gamma}}(\mathrm{i}\nu_n)$ in (17) and in (16) are identical. They may be obtained by matrix inversion in Matsubara frequency space

$$\frac{1}{\beta}\underline{\underline{\Gamma}}(\mathrm{i}\nu_n) = [\underline{\underline{\chi}}_{loc}]^{-1} - \beta[\underline{\underline{\Pi}}_{loc}(\mathrm{i}\nu_n)]^{-1} \qquad (18)$$

once the free local pp-Green function

$$\chi_{loc}(\mathrm{i}\omega_n, \mathrm{i}\omega_m; \mathrm{i}\nu_n) = G(\mathrm{i}\omega_n + \mathrm{i}\nu_n)G(-\mathrm{i}\omega_n)\delta_{\mathrm{i}\omega_n, \mathrm{i}\omega_m} \quad (19)$$

and the local pp-Green function $\underline{\underline{\Pi}}_{loc}(\mathrm{i}\nu_n)$ are known.

2.2.3 Local two-particle green function

The local two-particle f-Green function $\Pi_f(\mathrm{i}\omega_n, \mathrm{i}\omega_m; \mathrm{i}\nu_n)$ for the periodic Anderson model has been calculated within the NCA in the limit of two local valence configurations, one with N electrons and one with $N+1$ electrons [40]. For the two-channel model, the diagrammatic contribution is shown in Figure 2 and reads:

$$\Pi_f(\mathrm{i}\omega_n, i\omega_m; \mathrm{i}\nu_n)^{\alpha'\sigma;\alpha\sigma'}_{\alpha\sigma;\alpha'\sigma'} =$$
$$-\frac{1}{\tilde{Z}_{eff}}\oint_{\mathcal{C}} P_{-\alpha}(z)P_\sigma(z + \mathrm{i}\omega_n + \mathrm{i}\nu_n)$$
$$\times P_{-\alpha'}(z + \mathrm{i}\omega_n - i\omega_m)P_{\sigma'}(z - i\omega_m) \quad (20)$$

where the contour circumvents all singularities of the ionic propagators $P_\gamma(z)$. $\tilde{Z}_{eff}$ is the partition function of the effective site. The indices on the bottom of Π_f label the spin and channel of the incoming while the indices on the top label the outgoing particle-hole pair. Since there is one external line crossings when Π_f^{pp} is inserted into the Bethe-Salpeter equation (17), the overall sign must be negative.

In general, equation (20) has to be numerically evaluated. At $T = 0$, however, this integral can be solved analyticly for $|\mathrm{i}\omega_n| \ll \Delta$ for the two-channel Anderson model if we use the ionic propagators [41], assuming that the lattice self-consistency does not change the low-frequency threshold behaviour. This is justified in the paramagnetic phase for an energy independent DOS close to $\omega = 0$. A rather complicated calculation [27] yields

$$\Pi_f(\mathrm{i}\omega_n, \mathrm{i}\omega_m; 0) \approx \left(\frac{\pi}{4\Delta}\right)^2 \frac{\mathrm{sign}(\omega_n)\mathrm{sign}(\omega_m)}{|\max(\omega_n, \omega_m)|}$$
$$\times F\left(\frac{\pi}{2}; \left|\frac{\min(\omega_n, \omega_m)}{\max(\omega_n, \omega_m)}\right|\right), \quad (21)$$

where $F(\frac{\pi}{2}, x < 1)$ is the elliptic integral of the first kind. For low frequencies $\mathrm{i}\omega_n$ and $\mathrm{i}\omega_m$, $\Pi_f(\mathrm{i}\omega_n, \mathrm{i}\omega_m; 0)$ turns out to be independent of the low energy scale T_K. The conduction electrons over-screen the local spin: a compensation of the spin can never be achieved, and the conduction electrons continue to be incoherently scattered for $T \to 0$. The two-particle scattering is governed by low lying excitations independent of the cross-over energy scale T_K, and the temperature T appears to be the only relevant energy scale. This approximation is valid for $|\omega|, T < T_K$.

Since the large Coulomb repulsion prevents the ionic shell from accepting or donating two electrons at the same time, a local pair correlation at site i can only be generated sequentially. The first electron has to leave the f-shell before another conduction electron can enter it, see Figure 2. Therefore, the particle-particle f-Green function tends to have nodes as a function of time. $\Pi_f(\mathrm{i}\omega_n, \mathrm{i}\omega_n; 0)$ becomes an odd function of both of its frequency arguments $\mathrm{i}\omega_n$ and $\mathrm{i}\omega_m$ in the two-channel model due to the two exchangeable doublets. In other models with locally restricted charge fluctuations, we expect that odd and even components with respect to frequency will be present.

The periodic Anderson model contains two types of electrons: localized and itinerate ones. Since the bands are non-interacting in the absence of hybridization, particle-particle correlations only occurs through hybridization with localized states in ionic shells. We can express the conduction-band particle-particle Green function in DMFT as

$$\Pi_c(\mathrm{i}\omega_n, \mathrm{i}\omega_m; \mathrm{i}\nu_n) = \beta\chi_{c,loc} + \tilde{\chi}_{c,loc}\mathcal{T}_{loc}\tilde{\chi}_{c,loc}, \qquad (22)$$

where energy arguments have been dropped on the r.h.s. The local two-particle T-matrix $\mathcal{T}_{loc}^{(ph)}$ cumulant is defined by

$$\mathcal{T}_{loc}(\mathrm{i}\omega_n, \mathrm{i}\omega_m; \mathrm{i}\nu_n) = V^4(\Pi_f(\mathrm{i}\omega_n, \mathrm{i}\omega_n; \mathrm{i}\nu_n)$$
$$- \beta F(-\mathrm{i}\omega_n)F(\mathrm{i}\nu_n + \mathrm{i}\omega_n)\delta_{n,m}).$$
$$(23)$$

$\chi_{c,loc}(\mathrm{i}\omega_n, \mathrm{i}\omega_m; \mathrm{i}\nu_n) = \delta_{n,m}G_c(-\mathrm{i}\omega_n)G_c(\mathrm{i}\omega_n + \mathrm{i}\nu_n)$, and the media particle-particle Green function is

$$\tilde{\chi}_{c,loc} = \tilde{G}(-\mathrm{i}\omega_n)\tilde{G}(\mathrm{i}\omega_n + \mathrm{i}\nu_n).$$

Π_f factorizes in a product of two f-Green functions in the absence of local interactions, and the two-particle T-matrix cumulant vanishes as expected. Using equation (18) and (22) we obtain

$$\frac{1}{\beta}\underline{\underline{\Gamma}}_c = \underline{\underline{A}}\frac{1}{\beta}\underline{\underline{\mathcal{T}}}_{loc}\underline{\underline{A}}\frac{1}{1 + \underline{\underline{\tilde{\chi}}}_{c,loc}\frac{1}{\beta}\underline{\underline{\mathcal{T}}}_{loc}\underline{\underline{A}}} \qquad (24)$$

$$\underline{\underline{A}} = \underline{\underline{\tilde{\chi}}}_{c,loc}\,[\underline{\underline{\chi}}_{c,loc}]^{-1}. \qquad (25)$$

The matrix $\underline{\underline{A}}$ measures the degree of renormalization of the band electrons. It is of order $O(1)$ at high temperatures and becomes moderately enhanced in the low temperature regime. Hence, the irreducible vertex $\underline{\underline{\Gamma}}_c \approx \underline{\underline{\mathcal{T}}}_{loc}$. If we define a renormalized T-matrix $\underline{\underline{\tilde{\mathcal{T}}}}_{loc} = \underline{\underline{A}}\,\underline{\underline{\mathcal{T}}}_{loc}\,\underline{\underline{A}}$, the irreducible vertex assumes the same structure as the one-particle self-energy $\Sigma_{\alpha\sigma}^{(c)}(z)$ (6)

$$\underline{\underline{\Gamma}}_c = \underline{\underline{\tilde{\mathcal{T}}}}_{loc}\left[\underline{\underline{1}} + \underline{\underline{\chi}}_{c,loc}\underline{\underline{\tilde{\mathcal{T}}}}_{loc}\right]^{-1}. \qquad (26)$$

3 Superconductivity

3.1 Classification of the Cooper-pair operators

It is assumed that only the electrons in the conduction electron sub-system are directly involved in the formation of Cooper pairs in the condensed phase. The quantum numbers γ and γ' label their spin and orbital degrees of freedom. If a Cooper pair has an internal structure modelled by a structure factor $S(2\boldsymbol{r})$, its pair operator reads

$$P_{\gamma,\gamma'}(\boldsymbol{R}) = \sum_{\boldsymbol{r}} S(2\boldsymbol{r})c_\gamma(\boldsymbol{R}-\boldsymbol{r})c_{\gamma'}(\boldsymbol{R}+\boldsymbol{r}). \qquad (27)$$

$\boldsymbol{r} = (\boldsymbol{r}_1 - \boldsymbol{r}_2)/2$ determines the location of one electron relative to the center of mass $\boldsymbol{R} = (\boldsymbol{r}_1 + \boldsymbol{r}_2)/2$. The transformed pair operator $P_{\gamma,\gamma'}(\boldsymbol{q})$

$$P_{\gamma,\gamma'}(\boldsymbol{q}) = \sum_{\boldsymbol{k}} S(\boldsymbol{k})c_\gamma(\boldsymbol{k}-\boldsymbol{q}/2)c_{\gamma'}(-\boldsymbol{k}-\boldsymbol{q}/2) \qquad (28)$$

describes a pair in reciprocal space with a center of mass momentum $\boldsymbol{q}$.

Since in DMFT the irreducible particle-particle (pp) vertex Γ is also a $\boldsymbol{q}$-independent quantity, compare equation (9) to (12), the pair susceptibility

$$\chi_{p,\gamma,\gamma',\gamma'',\gamma'''}(\boldsymbol{q},\tau) = \left\langle T(P_{\gamma,\gamma'}(\boldsymbol{q})(\tau)P_{\gamma'',\gamma'''}^\dagger(\boldsymbol{q}))\right\rangle, \quad (29)$$

is only influenced by the local interaction if the structure factor $S(\boldsymbol{k})$ transforms with Γ_1, the trivial representation of the point group. Hence, solely superconducting instabilities with a conventional order parameter which also transforms according to Γ_1 can be obtained within DMFT through (29). This includes, however, Cooper pair form-factors such as $S(\boldsymbol{k}) \propto \varepsilon_{\boldsymbol{k}}$, sometimes called *extended s-wave*, which will play the leading role in the extreme mixed

Table 1. Classification of the 16 possible order parameters for local Cooper pairs. Pauli's principle determines the frequency behaviour of the symmetrized anomalous Green function $F(z)$. Odd frequency implies $(F(z) = -F(-z))$, even frequency $F(z) = F(-z)$. Only Cooper pairs with $S(\boldsymbol{k})$ transforming according to the irreducible representations Γ_1 are taken into account. Sector I and IV show odd frequency behaviour, while in sector II and III conventional even frequency pairing is found.

Sector	Spin	Channel	Frequency	# Orderp.
I (SsCs)	singlet	singlet	odd	1
II (SsCt)	singlet	triplet	even	3
III (StCc)	triplet	singlet	even	3
IV (StCt)	triplet	triplet	odd	9

valent regime where $\varepsilon_{\alpha\sigma} = 0$. Therefore, we will ignore unconventional spatial form factor symmetries which, of course, cannot be ruled out in the model.

The corresponding one-particle anomalous Green function $F_{\gamma,\gamma'}(\boldsymbol{k},\boldsymbol{q},z)$ is given by the Fourier transform of

$$F_{\gamma,\gamma'}(\boldsymbol{k},\boldsymbol{q},\tau) = -\left\langle T(c_{\gamma,\boldsymbol{k}-\boldsymbol{q}/2}(\tau)c_{\gamma',-\boldsymbol{k}-\boldsymbol{q}/2})\right\rangle, \qquad (30)$$

where $\boldsymbol{q}$ denotes the momentum of the Cooper pair.

Since γ contains the spin and orbital degrees $\sigma\alpha$, the possible symmetry properties of the pair susceptibility can be assigned to the four sectors listed in Table 1. These are associated with certain subspaces of the product space of spin and channel degrees of freedoms. Each of them are spanned by a product of singlet and triplet states as indicated. Since the total symmetry under exchange of the electrons has to be odd due to Pauli's principle, the frequency dependence of the symmetrized anomalous Green function $F(\boldsymbol{q},i\omega_n)$

$$F(\boldsymbol{q},i\omega_n) = \sum_{\gamma\gamma'\boldsymbol{k}} \lambda_{\gamma\gamma'}S(\boldsymbol{k})F_{\gamma,\gamma'}(\boldsymbol{k},\boldsymbol{q},i\omega_n) \qquad (31)$$

has to be odd in sector I and IV; hereby, $\lambda_{\gamma\gamma'}$ denotes the symmetry form-factor of the appropriate sector.

The most general pair operator in $\boldsymbol{k}$-space in sector I (spin singlet/channel singlet) is given by

$$P^{ss}(\boldsymbol{k},\boldsymbol{k}') = S\left(\frac{\boldsymbol{k}+\boldsymbol{k}'}{2}\right)\sum_{\alpha\sigma}\alpha\sigma c_{\boldsymbol{k}\alpha\sigma}c_{-\boldsymbol{k}'-\alpha-\sigma}, \qquad (32)$$

from which a symmetrized pair operator of the form (28) can be obtained by

$$P^{ss}(\boldsymbol{q}) = \sum_{\boldsymbol{k}} P^{ss}(\boldsymbol{k}+\boldsymbol{q}/2,\boldsymbol{k}-\boldsymbol{q}/2). \qquad (33)$$

When we introduce the transposed bi-spinor operator $\boldsymbol{\psi}^T(\boldsymbol{k}) = (c_{\boldsymbol{k}+\uparrow},c_{\boldsymbol{k}+\downarrow},c_{\boldsymbol{k}-\uparrow},c_{\boldsymbol{k}-\downarrow})$, the general pair operator in sector II (spin singlet/channel triplet) can be written as

$$\boldsymbol{P}^{s,t}(\boldsymbol{k},\boldsymbol{k}') = S(\frac{\boldsymbol{k}+\boldsymbol{k}'}{2})\boldsymbol{\psi}^T(\boldsymbol{k})i\underline{\underline{\sigma}}_y\,i\underline{\underline{\tau}}_y\underline{\underline{\boldsymbol{\tau}}}\boldsymbol{\psi}(-\boldsymbol{k}') \qquad (34)$$

and as

$$\boldsymbol{P}^{t,s}(\boldsymbol{k}, \boldsymbol{k}') = S(\frac{\boldsymbol{k} + \boldsymbol{k}'}{2})\boldsymbol{\psi}^T(\boldsymbol{k})\mathrm{i}\underline{\underline{\tau}}_y \, \mathrm{i}\underline{\underline{\sigma}}_y\underline{\underline{\boldsymbol{\sigma}}}\boldsymbol{\psi}(-\boldsymbol{k}') \qquad (35)$$

in sector III (spin triplet/channel singlet), where $\underline{\underline{\boldsymbol{\sigma}}}$ acts in the spin sector and $\underline{\underline{\tau}}$ in the channel sector. The nine pair operators of sector IV (spin and channel triplet) are given by the matrix with the elements

$$P_{i,j}^{t,t}(\boldsymbol{k}, \boldsymbol{k}') = S\left(\frac{\boldsymbol{k} + \boldsymbol{k}'}{2}\right)\boldsymbol{\psi}^T(\boldsymbol{k})\mathrm{i}\underline{\underline{\sigma}}_y\underline{\underline{\sigma}}_i \, \mathrm{i}\underline{\underline{\tau}}_y\underline{\underline{\tau}}_j\boldsymbol{\psi}(-\boldsymbol{k}). \tag{36}$$

3.2 Introduction to odd-frequency pairing

In Section 2.2.3, it was shown that the irreducible vertex Γ is proportional to the local f-particle-particle propagator Π_f in leading order, and that Π_f is odd in the incoming and outgoing frequencies at low temperatures, equation (21). Hence, we expect to find a tendency towards so-called odd-frequency superconductivity in model (1).

Berezinskii has pointed out in the context of ^{3}He that s-wave/spin triplet or p-wave/spin singlet pairing, both having a temporal node, are also compatible with Pauli's principle [23]: it only requires a total parity of -1. The anomalous Green function has to be an odd function, with respect to frequency, in the above mentioned cases. However, it quickly became apparent that ^{3}He orders in p-wave ($L = 1$), spin triplet ($S = 1$) pairs which show even frequency behaviour. Berezinskii's idea was forgotten, but was later revitalized by Balatsky et al. [42] in the context of superconducting phases of the Hubbard-model. Similar to magnetic phases, a superconduction ordered phase can have an order parameter whose modulation in real space is described by a finite wave vector $\boldsymbol{q}$. This wave vector corresponds to a finite center of mass momentum $\boldsymbol{q}$ of the Cooper pairs. Coleman et al. [43] investigated the possibility of an odd-frequency solution for a Kondo lattice model and found a stable solution for such a staggered order parameter within a mean-field theory. This solution, however, breaks spin-rotational invariance. The order parameter consists of a local spin contribution bound to a conduction electron and transforms as an $S = 1/2$ object. Abrahams et al. [44] argued that the order parameter of an odd-frequency superconductor has to be a composite object, i.e. a Cooper pair bound to a localized spin, in order to produce a positive Meissner effect. Therefore, time reversal symmetry is not broken by odd-frequency pairing since both components of the order parameter, the Cooper pair and the spin operator, have negative parity with respect to the time-reversal operator. Heid, however, showed that odd-frequency superconductors are thermodynamically instable against $\boldsymbol{q}$-modulation [25]. He assumed that the normal-phase was described by Fermi-liquid theory and that the order parameter did not have singularities. Emery and Kivelson [35] found an enhancement of a composite pair operator susceptibility using the solution of the two-channel Kondo-model at the Toulouse point. This

could indicate a tendency towards an odd-frequency phase in a corresponding lattice model.

Since the mechanism of superconductivity in strongly correlated electron systems is still subject to an ongoing debate, it is of great importance to explore this unusual concept in particular since, as will be seen below, it is favoured by orbital degrees of freedom. Whether odd-frequency pairing is actually realized in nature, is not yet clear.

3.3 Composite order parameter and its physical interpretation

Pauli's principle demands that superconductivity in the spin singlet, channel singlet (SsCs) sector or in the spin triplet, channel triplet (StCt) with a Γ_1 form-factor must have an odd anomalous Green function as indicated in Table 1. Assuming pairing with $\boldsymbol{q} = 0$, the local pair expectation value

$$\langle P_{ss}(\boldsymbol{q} = 0)\rangle = \frac{1}{N}\sum_{\boldsymbol{k}}\sum_{\alpha\sigma}\alpha\sigma S(\boldsymbol{k})\langle c_{\boldsymbol{k}\alpha\sigma}c_{-\boldsymbol{k}-\alpha-\sigma}\rangle = 0 \tag{37}$$

vanishes with the anti-commutator $\{c_{\boldsymbol{k}\alpha\sigma}, c_{-\boldsymbol{k}-\alpha-\sigma}\} = 0$, which reflects Pauli's principle. Hence, this expectation value cannot serve as the superconducting order parameter of Sections 1 and 4. This is a peculiarity of odd-frequency superconductivity.

Abrahams et al. noticed that the time derivative $D_{\gamma\gamma'} = \langle\frac{\mathrm{d}}{\mathrm{d}\tau}c_\gamma(\tau)c_{\gamma'}\rangle$ is non-vanishing in the odd frequency superconducting phase and may possibly be furnished as an order parameter [44]. Since the time derivative operator does not change the symmetry of the spin and orbital part, the order parameter can still be classified according to the symmetry of the conduction band Cooper pairs listed in Table 1. This new kind of order parameter is formed by linear combinations of $D_{\gamma\gamma'}$, which will be called O below. The derivative $\frac{\mathrm{d}}{\mathrm{d}\tau}c_\gamma(\tau)$ is equivalent to the commutator $[H, c_\gamma(\tau)]$. In the case of the two-channel periodic Anderson model, $\frac{\mathrm{d}}{\mathrm{d}\tau}c_\gamma(\tau)c_{\gamma'}$ consists of a product of two operators: a conduction electron pair operator and a local magnetic or channel spin operator both generated by the hybridization term between the band electrons and the local f-states. Thus, one arrives at a composite order parameter, which correlates local and itinerant degrees of freedom: formation of band Cooper pairs is stimulated in the presence of a local pair resonating between definite spin and channel states with proper symmetry.

Since there is only one order parameter component O_{ss} in sector I, it must be a global singlet. The only possibility to generate a singlet from a vector operator such as the local f-spin $\boldsymbol{S}$ is to form a scalar product involving another vector operator in the spin space. It has to be the conduction electron pair operator $\boldsymbol{P}^{t,s}$ given by equation (35) which is a scalar in orbital and a vector in spin space:

$$O_{ss} = \mathrm{sign}(\Delta E)\left(\langle\boldsymbol{S}\,\boldsymbol{P}^{t,s}\rangle - \langle\boldsymbol{\tau}\,\boldsymbol{P}^{s,t}\rangle\right). \tag{38}$$

The second term in this expression, the first term's symmetrical counterpart, combines a local f-shell orbital spin $\boldsymbol{\tau}$ and a pair operator $\boldsymbol{P}^{s,t}$ which is a vector in orbital space and a scalar in spin space to form a global singlet. Both terms are expected to contribute since the Hamiltonian (1) models local fluctuations between spin and orbital doublets at each lattice site. In this way, the "pair-wave function" in sector I realizes correlations between the dynamics of the local spin and a conduction electron pair, which are compliant with Pauli's principle.

The dimensionless order parameter O_{ss} is invariant under particle-hole transformation and simultaneous exchange of the two local doublets. This is also a fundamental symmetry of the Hamiltonian. The exchange of spin and channel spin is compensated by the sign change of $\Delta E = E_\sigma - E_\alpha = \varepsilon_{\alpha\sigma}$ being independent of spin and channel in the absence of a magnetic field or lattice distortion. Hence, the superconducting order parameter is not dependent on whether the magnetic or the quadrupolar doublet has the lower energy. Moreover, the composite order parameter meets the objective that the superconducting state must bind local magnetic or orbital degrees of freedom in order to quench the residual entropy present in the two-channel model.

The pair operators which enter O_{ss} in equation (38) transform according to the irreducible representationss of sectors II and III. This reflects the fact that Pauli's principle allows that their expectation value may stay finite. Of course, the symmetry of the composite order parameter is determined by the scalar product as a whole and not by the symmetry of the individual operators; therefore, the order parameter transforms according to sector I. A simple mean field decoupling of O_{ss}, as given by

$$O_{ss} = \text{sign}(\Delta E)\left(\langle \boldsymbol{S}\rangle \langle \boldsymbol{P}^{t,s}\rangle - \langle \boldsymbol{\tau}\rangle \langle \boldsymbol{P}^{s,t}\rangle\right), \qquad (39)$$

would essentially treat the local and itinerant correlations as independent quantities and would have to be interpreted as a mixture of phases of sectors II and III rather then superconductivity in sector I. Correlations between the conduction band pairs and the local spin and orbital degrees of freedom are essential for generating the unusual phase in sector I. Nevertheless, this decoupling might still be a way to understand the experimentally observed coexistence of magnetism and superconductivity in certain uranium Heavy Fermion compounds. An antiferromagnetic spin order, in conjunction with superconductivity with a zero center of mass momentum of the Cooper pair, would translate into a modulated order parameter O_{ss}, with wave vector $\boldsymbol{q}$ given by the magnetic modulation vector. Alternatively, one could speculate about a finite momentum Cooper-pair [45] bound to a modulated spin or orbital ordered state in such a way that the total momentum of the order-parameter is zero.

With the definitions

$$D_{\sigma\sigma'}^{\alpha\alpha'} = \frac{1}{\beta}\sum_{\mathrm{i}\omega_n} \mathrm{e}^{\mathrm{i}\omega_n\delta}\mathrm{i}\omega_n G_{c_{\nu\alpha\sigma},c_{\nu\alpha'\sigma'}}(\mathrm{i}\omega_n) \qquad (40)$$

$$T_{\sigma\sigma'}^{\alpha\alpha'} = \frac{1}{N\beta}\sum_{\mathrm{i}\omega_n,\boldsymbol{k}} \mathrm{e}^{\mathrm{i}\omega_n\delta}\mathrm{i}\omega_n \varepsilon_{\boldsymbol{k}\alpha\sigma} G_{c_{\boldsymbol{k}\alpha\sigma},c_{-\boldsymbol{k}\alpha'\sigma'}}(\mathrm{i}\omega_n), \qquad (41)$$

it is straightforward to derive exact relations for the symmetrized order parameter for the singlet/singlet channel in the form

$$O_{ss} = \frac{|\Delta E|}{V^2}\underbrace{\sum_{\alpha\sigma}\alpha\sigma D_{\sigma-\sigma}^{\alpha-\alpha}}_{=D_{ss}} + \frac{\text{sign}(\Delta E)}{V^2}\underbrace{\sum_{\alpha\sigma}\alpha\sigma T_{\sigma-\sigma}^{\alpha-\alpha}}_{=T_{ss}} \quad (42)$$

using equations of motion as sketched in Appendix A. The order parameter has two contributions: the term D_{ss} describes an isotropic local Cooper pair, i.e. $S(\boldsymbol{k}) = 1$, while T_{ss} is formed by nearest neighbour pairs, i.e. $S(\boldsymbol{k}) = \varepsilon_{\boldsymbol{k}}/t$, sometimes called extended s-wave pairing. The $\boldsymbol{k}$-summation on the r.h.s. of (41) leaves $T_{\sigma\sigma'}^{\alpha\alpha'}$ finite since $G_{c_{\boldsymbol{k}\alpha\sigma},c_{-\boldsymbol{k}\alpha'\sigma'}}(\mathrm{i}\omega_n) \propto S(\boldsymbol{k})$ for the case of extended s-wave pairing.

The composite order parameter O_{ss} contains no natural distinction between isotropic and anisotropic pairs with a form-factor $\varepsilon_{\boldsymbol{k}}/t$. It is interesting to note that for the intermediate valence regime $|E_\sigma - E_\alpha| \to 0$, the nearest neighbour Cooper pairs with extended s-wave symmetry dominate since the first term on the r.h.s. of (42) vanishes for $|\Delta E| \to 0$. This can be interpreted as condensation of delocalized pairs. There will not only be nodes in frequency in this regime but also nodes in $\boldsymbol{k}$-space.

An exact equation similar to (42) can be derived for the tensor order parameter in the triplet-triplet sector

$$O_{ij} = \text{sign}(\Delta E)\left(\langle s_i P_j^{s,t}\rangle - \langle \tau_j P_i^{t,s}\rangle\right) \qquad (43)$$

$$= \frac{|\Delta E|}{V^2}D_{i,j} + \frac{\text{sign}(\Delta E)}{V^2}T_{ij}, \qquad (44)$$

where $i,j = x,y,z$, $i(j)$ indexes the spin(channel) space, $P_j^{s,t}$ or $P_i^{t,s}$ is a component of the singlet/triplet or triplet/singlet pairs (34, 35) and the symmetrized isotropic (D_{ij}) and nearest neighbour pair (T_{ij}) expectation values are obtained by the symmetrization rules (36) in combination with (40) and (41):

$$D_{ij}(T_{ij}) = \sum_{\sigma\sigma'}^{\alpha\alpha'} D_{\sigma\sigma'}^{\alpha\alpha'}(T_{\sigma\sigma'}^{\alpha\alpha'})[\mathrm{i}\underline{\underline{\sigma}}_y\,\underline{\underline{\sigma}}_i]_{\sigma\sigma'}[\mathrm{i}\underline{\underline{\tau}}_y\,\underline{\underline{\tau}}_j]_{\alpha\alpha'}. \quad (45)$$

3.4 Composite order parameter and pair-susceptibility

As explained above, the order parameter is formed by a composite operator combining a conduction band pair operator in singlet/triplet channel with a local spin or channel operator in the two odd-frequency sectors I and II. It measures the correlation between a local spin and a conduction electron pair. To verify the existence of such an unconventional phase in the model, it is necessary to either show that there is a self-consistent solution of the order parameter equation in the symmetry broken phase or search for divergences of the order parameter susceptibility $\chi_O(\boldsymbol{q}) = G_{O,O^\dagger}(\mathrm{i}\nu_n = 0, \boldsymbol{q})$. It is cumbersome, however, to obtain a tractable expression for $\chi_O(\boldsymbol{q})$ since it

involves a three-particle Green function due to the composite nature of O. On the other hand, equations (42) and (44) connect the expectation value of the order parameter to the derivative of the symmetrized pair operator $\frac{\mathrm{d}}{\mathrm{d}\tau}c_\gamma^\dagger(\tau)c_{\gamma'}^\dagger$ which takes the form $P_{\gamma\gamma'}^{odd}(\mathrm{i}\omega_n) = \mathrm{i}\omega_n c_\gamma(\mathrm{i}\omega_n)c_{\gamma'}(-\mathrm{i}\omega_n)$ in the Matsubara frequency space. Therefore, it is equivalent to investigate the pair susceptibilities

$$\chi_P(\boldsymbol{q}) = \frac{1}{\beta^2} \sum_{\mathrm{i}\omega_n, \mathrm{i}\omega_m} G_{P^{odd}(\mathrm{i}\omega_n), P^{\dagger\,odd}(\mathrm{i}\omega_m)}(\mathrm{i}\nu_n = 0, \boldsymbol{q}).$$

$$(46)$$

They are obtained from two-particle Green functions whose four external lines are connected to a frequency dependent and, in the case of *"extended s-wave"* $\boldsymbol{k}$-dependent vertex, generated by $P_{\gamma\gamma'}^{odd}(\mathrm{i}\omega_n)$ and $P_{\gamma\gamma'}^{\dagger\,odd}(\mathrm{i}\omega_m)$.

Up to now, all statements in Section 3 are exact and independent of any approximation. In the following, however, we will calculate the two-particle Green functions only within the DMFT. Knowing the irreducible particle-particle vertex $\underline{\Gamma}$ for the appropriate symmetry, and only considering isotropic pairs, the pair susceptibility reads in general

$$\chi_P(\boldsymbol{q}, \mathrm{i}\nu_n) = \frac{1}{\beta} \sum_{\mathrm{i}\omega_n \mathrm{i}\omega_m} \mathrm{i}\omega_n(-\mathrm{i}\omega_m) \left[\underline{\chi}(\boldsymbol{q}, \mathrm{i}\nu_n) \right.$$
$$\left. \times \frac{1}{\underline{1} - \frac{1}{\beta}\underline{\Gamma}(\mathrm{i}\nu_n)\underline{\chi}(\boldsymbol{q}, \mathrm{i}\nu_n)} \right]_{\mathrm{i}\omega_n \mathrm{i}\omega_m}. \quad (47)$$

Since $\underline{\Gamma}$ is local within the DMFT, only gap functions transforming according to Γ_1 symmetry can be investigated. All other symmetries would require a microscopic solution of the model beyond the DMFT or the restriction to simple BCS mean-field theories. Especially latter approaches almost always confirms the ansatz and the assumptions made at the beginning of the calculations, and, therefore, it is not clear to us whether real physical insight is gained.

The phase transition temperature T_c and the frequency dependence of the anomalous self-energy $\Phi(\mathrm{i}\omega_n)$ is obtained by solving the eigenvalue equation

$$\underline{M}|\lambda, M\rangle = \lambda|\lambda, M\rangle, \quad (48)$$

where the symmetric matrix $\underline{M}$ is defined as

$$\underline{M} = \sqrt{\underline{\chi}(\boldsymbol{q}, 0)} \frac{1}{\beta}\underline{\Gamma}(0)\sqrt{\underline{\chi}(\boldsymbol{q}, 0)}. \quad (49)$$

The divergent contribution to the pair susceptibility at $\mathrm{i}\nu_n = 0$, *i.e.*

$$\chi_P(\boldsymbol{q}) = \underbrace{\frac{1}{\beta}c_{\lambda_m}^2 \frac{1}{1 - \lambda_m}}_{P(\boldsymbol{q})} + \text{regular terms} \quad (50)$$

stems from the largest eigenvalue $\lambda_m \to 1$. Hereby, c_{λ_m} is given by $\langle\lambda|\sqrt{\underline{\chi}(\boldsymbol{q}, 0)}|\omega_n\rangle$ and $|w_n\rangle = (\cdots, \omega_n, \cdots)^T$ (see Appendix B for more details). This is the DMFT-analog to the Eliashberg equation in the standard theory of superconductivity and was first used by Jarrell and coworkers [13,20].

4 Results for the phase boundary

As discussed before, all two-particle Green functions are evaluated within DMFT in the paramagnetic phase using standard procedures [12,14]. The temperature T_c at which the pair susceptibility diverges defines the boundary between the paramagnetic and the superconducting phase, if it is the highest instability temperature.

4.1 Sector I: Spin singlet/channel singlet (SsCs)

The pair operator in the odd-frequency SsCs sector

$$P_{ss}^{odd}(\boldsymbol{q}, \mathrm{i}\nu_n) = \frac{2}{\beta N} \sum_{\boldsymbol{k}\sigma \mathrm{i}\omega_n} \sigma \,\mathrm{i}\omega_n S(\boldsymbol{k})$$
$$\times c_{\boldsymbol{k}\sigma+}(\mathrm{i}\omega_n + \mathrm{i}\nu_n)c_{-\boldsymbol{k}+\boldsymbol{q}-\sigma-}(-\mathrm{i}\omega_n) \quad (51)$$

is derived from (32), where $S(\boldsymbol{k}) = 1$ for isotropic and $S(\boldsymbol{k}) = \varepsilon_{\boldsymbol{k}}/V$ of *"extended s-wave"* pairs. Hence, the pair susceptibility χ_P^{ss} consists of a spin diagonal and a spin or channel flip contribution. Now, the spin and channel indices, which have been neglected in Section 2.2.2 in order to focus on the structure rather than on details, are of importance: the resulting coupled Bethe-Salpeter equations yield

$$\chi_P^{\mathrm{SsCs}}(\boldsymbol{q}) = -\frac{8}{\beta^2} \sum_{\mathrm{i}\omega_n \mathrm{i}\omega_m} \mathrm{i}\omega_n \mathrm{i}\omega_m [\Pi^{dir}(\mathrm{i}\omega_n, \mathrm{i}\omega_m; \boldsymbol{q}, 0)$$
$$- \Pi^{ex}(\mathrm{i}\omega_n, \mathrm{i}\omega_m; \boldsymbol{q}, 0)] \quad (52)$$

in the absence of a magnetic field and isotropic Cooper-pairs. Π^{dir} describes spin and channel diagonal particle-particle propagation; Π^{ex} the exchange of spin or channel index. The coupled equations are solved for the particle-particle Green function $\Pi^{ss} = \Pi^{dir} - \Pi^{ex}$ from which the effective pp-vertex $\underline{\Gamma}^{ss}$ entering (47–49)

$$\frac{1}{\beta}\underline{\Gamma}^{ss} = \left[\underline{\chi}_{loc}\right]^{-1} - \beta\left[\underline{\Pi}_{loc}^{dir} - \underline{\Pi}_{loc}^{ex}\right]^{-1} \quad (53)$$

$$\chi_{loc}(\mathrm{i}\omega_n, \mathrm{i}\omega_m) = \delta_{n,m}G_c(\mathrm{i}\omega_n)G_c(-\mathrm{i}\omega_n) \quad (54)$$

is obtained for the singlet/singlet sector, where G_c denotes the conduction electron Green function.

Jarrell *et al.* investigated the pair susceptibility for the two-channel Kondo model in the strong coupling limit using QMC [13]. They did not find a maximum positive eigenvalue λ_m with $\lambda_m(T_c) = 1$ for a given finite temperature for $\boldsymbol{q} = 0$ or $\boldsymbol{q} = \pi(1, 1, 1)$ which is equivalent
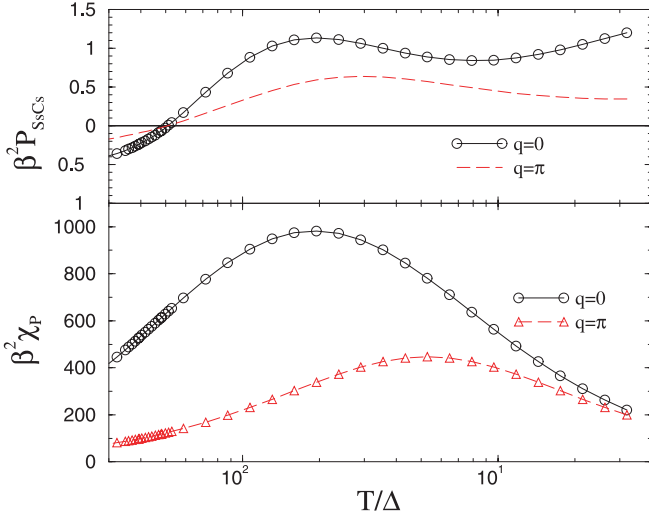
Fig. 3. Contribution P^{SsCs} to the pair susceptibility $\chi_P^{\text{SsCs}}(\boldsymbol{q})$ from the dominant maximal eigenvalue $|\lambda|$ vs. temperature in the singlet/singlet (SsCs) sector for $\boldsymbol{q} = 0$ and $\boldsymbol{q} = \pi(1, 1, 1)$ (upper plot). The lower plot shows the total pair susceptibility χ_P given by equation (47). Parameters: $\varepsilon_{\alpha\sigma} = -3$ and $n_c = 2$.

to $\eta(\boldsymbol{q}) = -1$ (staggered pairing). However, they observed that a single eigenvalue λ approaches $-\infty$. By lowering the temperature further, the associated eigenvector, i.e. the symmetry form-factor, corresponds to a very large positive eigenvalue which decreases with decreasing temperature leading to a sign change of the contribution P_{CsSc} to χ_P^{SsCs} (see Fig. 3 of Ref. [13]). Since an eigenvalue $\lambda > 1$ was found, it was interpreted as an indicator for a possible superconducting instability using a linearized Eliashberg equation. The simultaneous sign change of the staggered and the $\boldsymbol{q} = 0$ contribution is clearly visible in Figure 3 of reference [13] which looks very similar to the upper plot in Figure 3. Since λ appears to jump suddenly to a value $\lambda > 1$, it has been interpreted as a locally driven first order phase transition [13]. The susceptibility corresponding to the composite order parameter χ_P^{SsCs}, which would indicate a true instability of the whole system, was not investigated.

In general, the local conduction-electron particle-particle Green functions are obtained from a local two-particle t-matrix equation analogous to the ph-Green function (22) for models with non-interacting conduction bands. The local connected part of the two-particle T-matrix cumulant is given by

$$\mathcal{T}_{loc}^{ss}(\mathrm{i}\omega_n, \mathrm{i}\omega_m) = V^2 \left(\Pi_f^{dir}(\mathrm{i}\omega_n, \mathrm{i}\omega_m; 0) - \Pi_f^{ex}(\mathrm{i}\omega_n, \mathrm{i}\omega_m; 0) \right.$$
$$\left. - \beta F(\mathrm{i}\omega_n) F(-\mathrm{i}\omega_n) \delta_{n,m} \right). \quad (55)$$

Within NCA, the spin or channel exchanging two-particle f-Green function Π_f^{ex}, depicted in Figure 2, is of the order of $O(v^0 = 1)$, where $v = V\rho$. However, the local two-particle f-Green function, diagonal in spin and channel indices, turns out to be of the order of $O(v^2)$ and, therefore, is neglected leading to a total contribution of $\Pi_f^{pp}(\mathrm{i}\omega_n, \mathrm{i}\omega_m; 0)$ given by (21). We solved the Eliashberg-like equation (48) and confirmed the results of Jarrell

et al. [13] for the two-channel periodic Anderson model. The temperature dependence of P^{SsCs}, depicted in the upper plot of Figure 3, shows excellent agreement with the published results for the two-channel Kondo model (see Fig. 3 of Ref. [13]).

In Appendix C, we show that the sign change of a contribution to the pair susceptibility is equivalent to finding a non-trivial solution to the linearized DMFT self-consistency condition (SCC) in the symmetry broken phase. This will be discussed later in Section 5.1.1 in more detail. However, the form factor which was found for the Kondo model [13] and the two-channel periodic Anderson model in our calculation appears to be singular at $\omega = 0$: $F(\omega) \propto 1/\omega$. This has the effect that a linearization of the DMFT equations, on which the linearized Eliashberg equation is based on, is not justified for $|\omega| \to 0$, and the full SCC has to be considered before any conclusion about the existence of a symmetry broken state can be drawn for sector I. Additionally, the susceptibility of the composite order parameter χ_P^{SsCs} is three orders of magnitude larger than the particular component P^{SsCs} exhibiting the sign change which, therefore, might be an irrelevant contribution to the total pair-susceptibility of the composite order parameter O_{ss}.

We investigated the SsCs sector for a large range of parameters and did not detect a phase transition or a sign change in χ_P^{SsCs}. The sign change of the contribution P^{ScCs} to χ_P^{SsCs} has been viewed as indication of a first order phase transition by Jarrell and coworkers [13]. However, we always find a higher transition temperature in the spin-triplet, channel triplet sector for the investigated parameters of the two-channel Anderson lattice model. We believe that the charge fluctuations on the f-shell plays a major role in the formation of the superconducting phase of the Anderson lattice model as can be seen from equations (42) and (44) while these charge fluctuations are absent in the Kondo-lattice model. The superconducting gap function is dominated by an so-called "extended s-wave" (Γ_1) form factor $S(\boldsymbol{k}) = \sum_\alpha \cos(k_\alpha)$ parameter in the extreme intermediate valence regime, $\Delta E = 0$.

4.2 Sector II (SsCt) and sector III (StCs)

We looked into the even frequency eigenspace of $\underline{\underline{\Gamma}}^{ss}$ (53) and $\underline{\underline{\Gamma}}^{tt}_{even}$

$$\frac{1}{\beta} \underline{\underline{\Gamma}}^{tt}_{even} = \underline{\underline{E}}_{even} \left(\left[\underline{\underline{\chi}}^{pp}_{loc} \right]^{-1} - \beta \left[\underline{\underline{\Pi}}^{dir}_{loc} + \underline{\underline{\Pi}}^{ex}_{loc} \right]^{-1} \right) \underline{\underline{E}}_{even}, \quad (56)$$

which belong to the StCs and the SsCt sector, respectively. $\underline{\underline{E}}_{even}|_{n,m} = (\delta_{n,m} + \delta_{m,n})/2$ projects out the odd-frequency components. No instability was found in either sector. This was expected from the analytic form of two-particle T-matrix (21) which is asymptotically odd in its frequency arguments (see also Sect. 2.2.3).
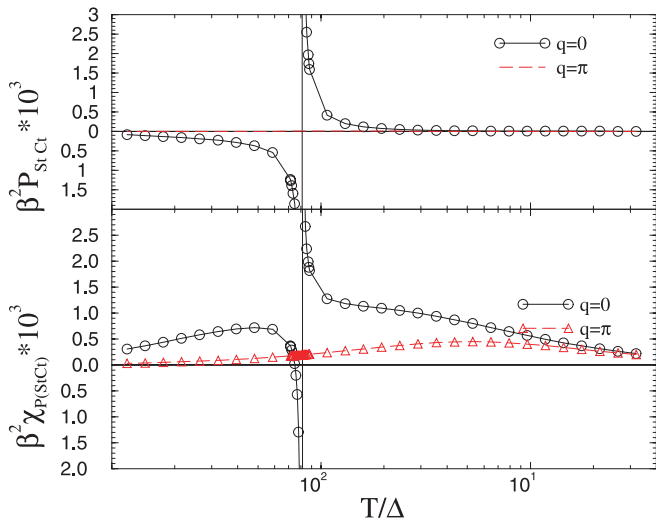
Fig. 4. Contribution P^{StCt} to the pair-susceptibility χ_P from the largest positive eigenvalue *vs.* temperature in the triplet/triplet (StCt) sector for $\boldsymbol{q} = \pi(1,1,1)$ (staggered) and $\boldsymbol{q} = 0$ (upper plot), and total pair-susceptibility χ_P, equation (52), *vs.* temperature (lower plot). Parameters: $\varepsilon_{\alpha\sigma} = -3$ and $n_c = 2$.

4.3 Sector IV: Spin triplet/channel triplet (StCt)

The spin triplet, channel triplet sector, StCt, is characterized by a tensor order parameter with nine components (44) (see also Tab. 1). Some of the two-particle Green functions in this sector involve both a direct and an exchange contribution yielding a matrix representation in Matsubara frequency space which shows an odd-frequency dependence in order to obey Pauli's principle, for example: the spin and channel diagonal Green function. This structure is already revealed in the free local particle-particle Green function

$$\chi_{loc}^{\sigma\alpha}(\mathrm{i}\omega_n, \mathrm{i}\omega_m; \mathrm{i}\nu_n) = G_{\sigma\alpha}(\mathrm{i}\omega_n + \mathrm{i}\nu_n)G_{\sigma\alpha}(-\mathrm{i}\omega_n)$$
$$\times (\delta_{n,m} - \delta_{-\mathrm{i}\omega_n, \mathrm{i}\omega_m + \mathrm{i}\nu_n}) \quad (57)$$

for $\mathrm{i}\nu_n = 0$. Consequently, the matrix inversion is mathematically ill-defined in the particle-particle version of equation (26) since the determinant of an odd matrix in Matsubara frequency space must vanish. This problem can be circumvented by defining a matrix inversion for odd-frequency matrices in relation to an odd frequency unitary matrix $E_{odd}(n,m) = (\delta_{n,m} - \delta_{n,-m})/2$. This analysis, however, is only necessary for some of the nine different pp-Green functions which are needed for the diagonal order parameter susceptibilities $\chi_{P,ij}^{\mathrm{StCt}} = G_{O_{ij}, O_{ij}^\dagger}(0)$. By careful analysis of all triplet two-particle Green functions, it can be shown that all odd-frequency pair-susceptibilities are equal in DMFT, and the relevant irreducible vertex is given by

$$\frac{1}{\beta}\underline{\underline{\Gamma}}^{tt} = \underline{\underline{E}}_{odd}\left(\left[\underline{\underline{\chi}}_{loc}^{pp}\right]^{-1} - \beta\left[\underline{\underline{\Pi}}_{loc}^{dir} + \underline{\underline{\Pi}}_{loc}^{ex}\right]^{-1}\right)\underline{\underline{E}}_{odd},$$

$$(58)$$

where $\underline{\underline{E}}_{odd}$ projects out the odd-frequency components.

For the two-channel Kondo-lattice model, $\chi_{P,zz}^{\mathrm{StCt}}$ was investigated by Jarrell *et al.* [13], and no superconducting instability was found for Kondo couplings of $J/t \geq 0.4$. A different picture emerges in the two-channel periodic Anderson model. In Figure 4, the total pair-susceptibility χ_P^{StCt} (lower curves) and the contribution stemming from the largest eigenvalue P^{StCt} (upper curves) are shown in the stable moment regime for half-filling and for the center of mass momenta $\boldsymbol{q} = 0$ and $\boldsymbol{q} = \pi(1,1,1)$. A sign change is observed in both quantities at a temperature of $T \approx 8 \times 10^{-3}\Delta$ and for $\boldsymbol{q} = 0$, which originates from the divergence of P_{StCt} as $\lambda_{\max} \to 1$. Consequently, we find a clear tendency towards a second order phase transition in the triplet/triplet sector for an uniform order parameter. The pair-susceptibility of a staggered pair is much smaller than $\chi_P^{\mathrm{StCt}}(\boldsymbol{q} = 0)$ and stays continuous in the vicinity of T_c. The qualitative difference of the Kondo-lattice model and periodic Anderson model is the possibility of change fluctuation on the f-shell in the latter model, which is not possible in the first.

The characteristic temperature of the lattice, T^*, was phenomenologically defined as the temperature at which the ratio of effective local moment $\mu_{eff}^2(T) = T\chi_{loc}(T)$ and the free moment $\mu_{free}^2 = \lim_{T\to\infty}\mu_{eff}^2(T)$ equal 0.4: $\mu_{eff}^2(T^*)/\mu_{free}^2 = 0.4$. $\chi_{loc}(T)$ is the local susceptibility of the ground state spin. Therefore, T^* is a measure of the Kondo screening of the local magnetic or quadrupolar spin.

We investigated the pair-susceptibility χ_P^{StCt} in the intermediate valence, the Kondo and the stable moment regime for band-fillings between quarter and 3/4-filling and COM momentum of $\boldsymbol{q} = 0$ and $\boldsymbol{q} = \pi(1,1,1)$. We always performed a finite size scaling analysis for the largest eigenvalue of $\underline{\underline{M}}$, equation (49), with respect to the matrix size: λ_m approaches a constant for $30-40$ Matsubara frequencies. The superconductivity is driven by the low energy components of the two-particle vertex in contrary to the magnetic phase transitions [14] where $400-500$ Matsubara frequencies are needed in order to obtain a susceptibility invariant of the size of the matrix. A superconducting transition was always obtained, but only for $\boldsymbol{q} = 0$. Although T_c decreases with decreasing coupling constant $g = \rho_0 J = \Delta/|\varepsilon_{\alpha\sigma}|$, the normalized transition temperature $t_c = T_c/T^*$ shown an increase due to the exponential sensitivity of T^* on g as depicted in Figure 5a. T^* decreases away from half-filling $n_c > 2$: hence t_c increases with n_c as shown in Figure 5b. The asymmetry of T^* as function of n_c simply stems from the asymmetry of energy of the two local doublets. This asymmetry disappears for $\varepsilon_{\alpha\sigma} = 0$.

The odd-frequency vertex is attractive (repulsive) in the StCt (SsCs) sector as seen analytically in the weak coupling limit $V \to 0$ from (24, 53) and (58) in combination with an NCA approximation for $\Pi_f^{pp}(\mathrm{i}\omega_n, \mathrm{i}\omega_m; 0)$ given by (21).
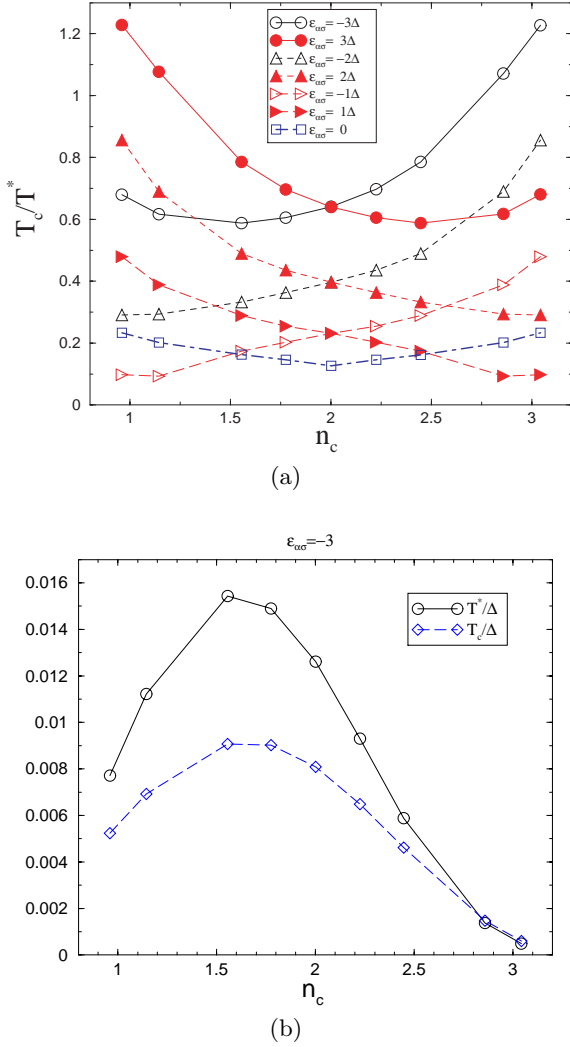
(a)

(b)

Fig. 5. Reduced transition temperature $t_c = T_c/T^*$ (a) as a function of the band filling n_c for four different values of $|\varepsilon_{\alpha\sigma}|$ and (b) the dependence of T_c and T^* on n_c for $\varepsilon_{\alpha\sigma} = -3\Delta$. The components of superconducting order parameter O_{ij} are invariant under $\varepsilon_{\alpha\sigma} \to -\varepsilon_{\alpha\sigma}$ and a simultaneously performed particle-hole transformation, as can be clearly seen in the plot. Even though T_c increases for decreasing $|\varepsilon_{\alpha\sigma}|$, the ratio T_c/T^* decreases since increasing charge fluctuation tends to destabilize the superconductivity.

5 Dynamical mean field theory of the superconducting phase

We have established the phase boundary between the homogeneous, paramagnetic and the superconducting phase in Section 2.2.2. Only the one-particle and two-particle solutions of the effective site enter the calculation of the pair-susceptibility in paramagnetic phase. In this section, the modified DMFT equations for the superconducting phase are derived and approximately evaluated. New insight on the physical properties of this phase will be gained.

5.1 Green functions

The Greens function is an 8×8 matrix in the spin and orbital space and formally written as

$$\underline{\underline{G}}(\mathrm{i}\omega_n, \boldsymbol{k}) = \begin{pmatrix} \underline{\underline{E}}^{-1}(\mathrm{i}\omega_n, \boldsymbol{k}) & -\underline{\underline{\Phi}}(\mathrm{i}\omega_n, \boldsymbol{k}) \\ -[\underline{\underline{\Phi}}(-\mathrm{i}\omega_n, \boldsymbol{k})]^h & \underline{\underline{H}}^{-1}(\mathrm{i}\omega_n, \boldsymbol{k}) \end{pmatrix}^{-1}, \quad (59)$$

where $\underline{\underline{H}}^{-1}(\mathrm{i}\omega_n, \boldsymbol{k}) = -\underline{\underline{E}}^{-1}(-\mathrm{i}\omega_n, \boldsymbol{k})$. $\underline{\underline{E}}$ describes the electron, $\underline{\underline{H}}$ the hole propagation in the paramagnetic phase if $\underline{\underline{\Phi}} = 0$. The relation between the off-diagonal matrix elements is a consequence of the definition of the Green function and, therefore, is a fundamental relation independent of possible symmetries of the order parameter. $\underline{\underline{\Phi}}(\mathrm{i}\omega_n, \boldsymbol{k})$ is a 4×4 matrix in the combined spin/channel space containing 16 linear independent anomalous Green functions. Since the Hamiltonian conserves magnetic and channel spin, the natural decomposition is given by

$$\begin{aligned} \underline{\underline{\Phi}}(\mathrm{i}\omega_n, \boldsymbol{k}) &= \mathrm{i}\underline{\sigma}_2[\Phi_0^s(\mathrm{i}\omega_n, \boldsymbol{k})\underline{1} + \boldsymbol{\Phi_s}(\mathrm{i}\omega_n, \boldsymbol{k})\underline{\sigma}] \\ &\quad \times \mathrm{i}\underline{\tau}_2[\Phi_0^c(\mathrm{i}\omega_n, \boldsymbol{k})\underline{1} + \boldsymbol{\Phi_c}(\mathrm{i}\omega_n, \boldsymbol{k})\underline{\tau}] \\ &= -\underline{\sigma}_2\underline{\tau}_2 \big[\Phi_0^s(\mathrm{i}\omega_n, \boldsymbol{k})\Phi_0^c(\mathrm{i}\omega_n, \boldsymbol{k})\underline{1} \\ &\quad + \Phi_0^s(\mathrm{i}\omega_n, \boldsymbol{k})\underline{1}\boldsymbol{\Phi_c}(\mathrm{i}\omega_n, \boldsymbol{k})\underline{\tau} \\ &\quad + \Phi_0^c(\mathrm{i}\omega_n, \boldsymbol{k})\underline{1}\boldsymbol{\Phi_s}(\mathrm{i}\omega_n, \boldsymbol{k})\underline{\sigma} \\ &\quad + \boldsymbol{\Phi_s}(\mathrm{i}\omega_n, \boldsymbol{k})\underline{\sigma}\boldsymbol{\Phi_c}(\mathrm{i}\omega_n, \boldsymbol{k})\underline{\tau} \big], \quad (60) \end{aligned}$$

where $\underline{\tau}$ acts in channel space and $\underline{\sigma}$ in spin space. The anomalous components are given by the product $\Phi_0^s(\mathrm{i}\omega_n, \boldsymbol{k})\Phi_0^c(\mathrm{i}\omega_n, \boldsymbol{k})$ in the SsCs sector, $\Phi_0^s(\mathrm{i}\omega_n, \boldsymbol{k})\boldsymbol{\Phi_c}(\mathrm{i}\omega_n, \boldsymbol{k})$ in the SsCt sector, $\Phi_0^c(\mathrm{i}\omega_n, \boldsymbol{k})\boldsymbol{\Phi_s}(\mathrm{i}\omega_n, \boldsymbol{k})$ in the StCs sector and the tensor $T_{ij} = \Phi_i^s(\mathrm{i}\omega_n, \boldsymbol{k})\Phi_j^c(\mathrm{i}\omega_n, \boldsymbol{k})$ in the StCt sector. The similarities to He^3 are striking: in He^3 the order parameter is a tensor which also can be written as a product of spin and orbital functions. Focusing on the individual symmetry sector of interest, the spin/channel matrix product $\underline{\underline{\Phi}}(\mathrm{i}\omega_n, \boldsymbol{k})[\underline{\underline{\Phi}}(-\mathrm{i}\omega_n, \boldsymbol{k})]^h$ is obtained in the StCt sector

$$\begin{aligned} \underline{\underline{\Phi}}(\mathrm{i}\omega_n, \boldsymbol{k})[\underline{\underline{\Phi}}(-\mathrm{i}\omega_n, \boldsymbol{k})]^h &= \big(\boldsymbol{\Phi_c}(\mathrm{i}\omega_n, \boldsymbol{k})\boldsymbol{\Phi_c^*}(-\mathrm{i}\omega_n, \boldsymbol{k})\big) \\ &\quad \times \big(\boldsymbol{\Phi_s}(\mathrm{i}\omega_n, \boldsymbol{k})\boldsymbol{\Phi_s^*}(-\mathrm{i}\omega_n, \boldsymbol{k})\big)\underline{1} \\ &= \mathrm{Tr}\big[\underline{d}(\mathrm{i}\omega_n, \boldsymbol{k})\underline{\overline{d}}(-\mathrm{i}\omega_n, \boldsymbol{k})\big]\underline{1}, \end{aligned} \quad (61)$$

where we have introduced the a new parameter matrices

$$\begin{aligned} \underline{d}(\mathrm{i}\omega_n, \boldsymbol{k}) &= \boldsymbol{\Phi_s}(\mathrm{i}\omega_n, \boldsymbol{k})\boldsymbol{\Phi_c}^T(\mathrm{i}\omega_n, \boldsymbol{k}) \quad, \\ \underline{\overline{d}}(\mathrm{i}\omega_n, \boldsymbol{k}) &= \boldsymbol{\Phi_c^*}(\mathrm{i}\omega_n, \boldsymbol{k})\boldsymbol{\Phi_s^*}^T(\mathrm{i}\omega_n, \boldsymbol{k}) \quad (62) \end{aligned}$$

and restricted our search to "unitary states": $\boldsymbol{\Phi}_{c(s)}(\mathrm{i}\omega_n, \boldsymbol{k}) \times \boldsymbol{\Phi}_{c(s)}^*(-\mathrm{i}\omega_n, \boldsymbol{k}) = 0$ in obvious analogy to the treatment of He^3 [1]. Under the assumption

that only the StCt-sector becomes superconducting, the full 8×8 Greens function is then given by

$$
\begin{aligned}
\underline{G}(\mathrm{i}\omega_n, \boldsymbol{k}) = 4 \left(\mathrm{Tr} \left[\underline{E}^{-1}(\mathrm{i}\omega_n, \boldsymbol{k}) \underline{\underline{H}}^{-1}(\mathrm{i}\omega_n, \boldsymbol{k}) \right] \right. \\
-4 \mathrm{Tr} \left[\underline{d}(\mathrm{i}\omega_n, \boldsymbol{k}) \underline{\overline{d}}(-\mathrm{i}\omega_n, \boldsymbol{k}) \right] \Big)^{-1} \\
\times \left(\begin{array}{cc} \underline{\underline{H}}^{-1}(\mathrm{i}\omega_n, \boldsymbol{k}) & \underline{\Phi}(\mathrm{i}\omega_n, \boldsymbol{k}) \\ \left[\underline{\Phi}(-\mathrm{i}\omega_n, \boldsymbol{k}) \right]^h & \underline{E}^{-1}(\mathrm{i}\omega_n, \boldsymbol{k}) \end{array} \right)^{-1} .
\end{aligned} \tag{63}
$$

Without directional coupling between spatial and spin/orbit degrees of freedom, the tensor d_{ij} separates as

$$
\underline{d}(\mathrm{i}\omega_n, \boldsymbol{k}) = g(\mathrm{i}\omega_n, \boldsymbol{k}) \boldsymbol{n_s} \cdot \boldsymbol{n_c}^T, \tag{64}
$$

where $\boldsymbol{n_s}$ and $\boldsymbol{n_c}^T$ are constant unity vectors in spin and channel space, and an amplitude function $g(\mathrm{i}\omega_n, \boldsymbol{k}) = -g(-\mathrm{i}\omega_n, \boldsymbol{k})$. If the superconducting phase is chosen in such a way that g is a purely imaginary function of the arguments, and $g^*(-\mathrm{i}\omega_n, \boldsymbol{k}) = g(\mathrm{i}\omega_n, \boldsymbol{k})$ holds, we obtain the Nambu Green function as

$$
\underline{G}(\mathrm{i}\omega_n, \boldsymbol{k}) = [(\mathrm{i}\omega_n - \Sigma(\mathrm{i}\omega_n) - \varepsilon_{\boldsymbol{k}})(\mathrm{i}\omega_n + \Sigma(-\mathrm{i}\omega_n) + \varepsilon_{\boldsymbol{k}})
$$

$$
- g(\mathrm{i}\omega_n, \boldsymbol{k}) g(\mathrm{i}\omega_n, \boldsymbol{k})]^{-1}
$$

$$
\times \left(\begin{array}{cc} (\mathrm{i}\omega_n + \Sigma(-\mathrm{i}\omega_n) + \varepsilon_{\boldsymbol{k}}) \underline{\underline{1}} & g(\mathrm{i}\omega_n, \boldsymbol{k}) \underline{\sigma}_2 \underline{\tau}_2 \left[\boldsymbol{n_s} \underline{\sigma} \boldsymbol{n_c} \underline{\tau} \right] \\ g(\mathrm{i}\omega_n, \boldsymbol{k}) \left(\underline{\sigma}_2 \underline{\tau}_2 \left[\boldsymbol{n_s} \underline{\sigma} \boldsymbol{n_c} \underline{\tau} \right] \right)^h & (\mathrm{i}\omega_n - \Sigma(\mathrm{i}\omega_n) - \varepsilon_{\boldsymbol{k}}) \underline{\underline{1}} \end{array} \right) .
$$

We have reduced the 8×8 Nambu Green function-matrix to a standard 2×2 problem for the amplitude function $g(z, \boldsymbol{k})$ and the diagonal self-energy Σ with the above assumptions.

5.1.1 DMFT one-particle self-consistency condition

As shown in the previous section, the 8×8 Nambu Green function matrix can be reduced to a 2×2 matrix determining the dynamics of a homogeneous superconducting phase. In order to derive DMFT equations with a purely local self-energy matrix, the anomalous self-energy has to be restricted to isotropic pairs, $e.g.$ $S(\boldsymbol{k}) = 1$

$$
\underline{G}_c(z) = \frac{1}{N} \sum_{\boldsymbol{k}} \left[\left[\underline{G}_c^0(\boldsymbol{k}, z) \right]^{-1} - \underline{\Sigma}_c(z) \right]^{-1} \tag{66}
$$

$$
\left[\underline{\tilde{G}}_c(z) \right]^{-1} = \left[\underline{G}_c(z) \right]^{-1} + \underline{\Sigma}_c(z), \tag{67}
$$

where $\underline{\tilde{G}}_c(z)$ corresponds to the medium or dynamical mean field in which the effective impurity is embedded. It is related to a generalized Anderson width matrix by

$$
\underline{\underline{\Delta}}(z) = V^2 \underline{\sigma}_2 \underline{\tilde{G}}_c(z) \underline{\sigma}_2 \tag{68}
$$

and has normal and anomalous components describing quasi-particle propagation and pair-creation and annihilation, respectively. All components enter the calculation

of the effective impurity. The self-energy $\underline{\Sigma}_c(z)$ is determined via

$$
\underline{\Sigma}_c = \underline{\underline{T}} \left[\underline{\underline{1}} + \underline{\tilde{G}} \underline{\underline{T}} \right]^{-1}, \tag{69}
$$

a matrix generalization of the usual DMFT self-consistency equations, where the diagonal elements of the T-matrix are given by the local quasi-particle scattering matrices $T_e = T_{11}(z) = V^2 G_f(z)$ and $T_h = T_{22}(z) = -V^2 G_f(-z)$. The anomalous contribution is calculated from

$$
T_s = T_{12}(\mathrm{i}\omega_n) = -V^4 \frac{1}{\beta} \sum_{\mathrm{i}\omega_m} \Pi_f(\mathrm{i}\omega_n, \mathrm{i}\omega_m; 0) \tilde{f}(\mathrm{i}\omega_m). \tag{70}
$$

The negative sign takes into account that

$$
\Delta_{12}(z) = -V^2 \tilde{G}_{12}(z) = -V^2 \tilde{f}(z). \tag{71}
$$

5.2 Connection between the pair-susceptibility and Green function in the superconducting phase

The DMFT equations of the previous section are independent of the algorithm to obtain spectral information on the effective site. If $g(z) \rightarrow 0$ holds for all frequencies when $T \nearrow T_c$, the divergence of the pair-susceptibility, or finding an eigenvalue of $\lambda = 1$ for the matrix $\underline{\underline{M}}$, equation (48), is equivalent to solving (66) and (67) and

$$
g(\mathrm{i}\omega_n) = \frac{1}{\beta} \sum_{\mathrm{i}\omega_m} \Gamma_c(\mathrm{i}\omega_n, \mathrm{i}\omega_m) \chi_0(\boldsymbol{q} = 0, 0) g(\mathrm{i}\omega_m) \tag{72}
$$

is obtained ($| \lambda = 1 \rangle \propto g(\mathrm{i}\omega_n)$) as shown in Appendix C. As expected in a mean-field theory, the quasi-particle self-energies are not renormalized.

However, all eigenvectors with $\lambda = 1$ which lead to superconducting phase transitions reported in Section 4.3 show a $1/\mathrm{i}\omega_n$ behaviour in leading order reflecting the analytic properties of the irreducible vertex [27], equation (21). Therefore, the assumption of a simple second order phase transition with $|g(z)| \rightarrow 0$ does not hold, indicating that also the quasi-particle properties are strongly renormalized by entering the superconducting phase. The linearization of equations (66–69) with respect to $g(z)$ is not possible below T_c. This implies that Heid's theorem [25], which states that odd-frequency superconducting state is associated with a maximum in the free energy, does not apply to the triplet/triplet superconducting state. Its its derivation relies on the analyticity of $g(z)$ on the real axis. In general, $\underline{\Sigma}$ reads

$$
\underline{\underline{\Sigma}} = \frac{1}{A} \left(\begin{array}{cc} T_e + \tilde{h}(T_e T_h - T_s^2) & T_s - \tilde{f}(T_e T_h - T_s^2) \\ T_s - \tilde{f}(T_e T_h - T_s^2) & T_h + \tilde{e}(T_e T_h - T_s^2) \end{array} \right) \tag{73}
$$

$$
A = (1 + \tilde{e} T_e + \tilde{f} T_s)(1 + \tilde{h} T_h + \tilde{f} T_s)
$$

$$
- (\tilde{e} T_s + \tilde{f} T_h)(\tilde{h} T_s + \tilde{f} T_e), \tag{74}
$$

which implies the renormalization of the quasi-particle self-energy $\underline{\underline{\Sigma}}_{11}$ by the terms $-\tilde{h} T_s^2$ even if the we assume that the quasi-particle scattering t-matrices T_h and T_e are not renormalized close to T_c.
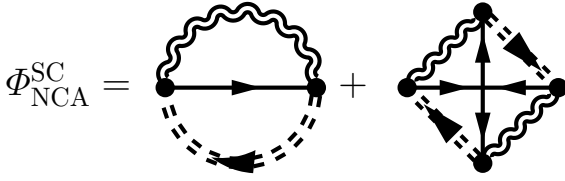
Fig. 6. Diagrammatic representation of the generating functional $\Phi_{\mathrm{NCA}}^{\mathrm{SC}}$ for the NCA in the superconduction (SC) phase: the first diagram is the normal contribution, the second one is the anomalous contribution. The wiggly lines represent the Green function P_α of the quadrupolar doublet, the dashed lines P_σ for the magnetic doublet and the solid lines are the appropriate components of the media Green function-matrix $\underline{\tilde{G}}$. The second term generates contributions to the self-energies of the ionic Green functions and the anomalous T-matrix.
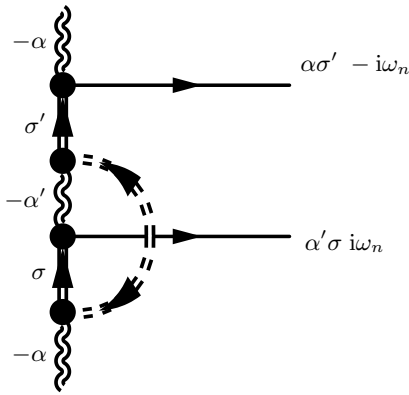
Fig. 7. Diagrammatic representation of the local anomalous T-matrix in NCA plotted on an imaginary time axis, from bottom to top. It was obtained by contracting the incoming lines of the diagram shown in Figure 2. The double dashed line represents anomalous Cooper-pair bath function $\tilde{f}(z)$ which obeys $\tilde{f}(z) = -\tilde{f}(-z)$.

5.3 Modified non-crossing-approximation for the superconducting phase

T_s is generated by the second term of the generating functional for the effective site in a superconducting medium depicted in Figure 6. The diagrammatic representation of T_s is shown in Figure 7. We have evaluated (70) in NCA by four integrals along the branch-cuts by convoluting the Cooper-pair media Green function $\tilde{f}(z)$ with $\Pi_f(\mathrm{i}\omega_n, \mathrm{i}\omega_m; 0)$, equation (20). It was shown that the instability in χ_P brings forth a solution of (67–70) when expanded linearly in the anomalous Green functions and medium (see also Appendix C).

Since we cannot use a linearized version of the DMFT close to T_c as discussed in the previous section, we iterated the full DMFT for the superconducting phase, equations (67–70), without any further approximations for $1 - T/T_c \ll 1$. The generating functional of the effective site $\Phi_{\mathrm{NCA}}^{\mathrm{SC}}$ is shown in Figure 6. For $T > T_c$, the equations are identical to the normal state DMFT since $g(z)$ iterates to zero.
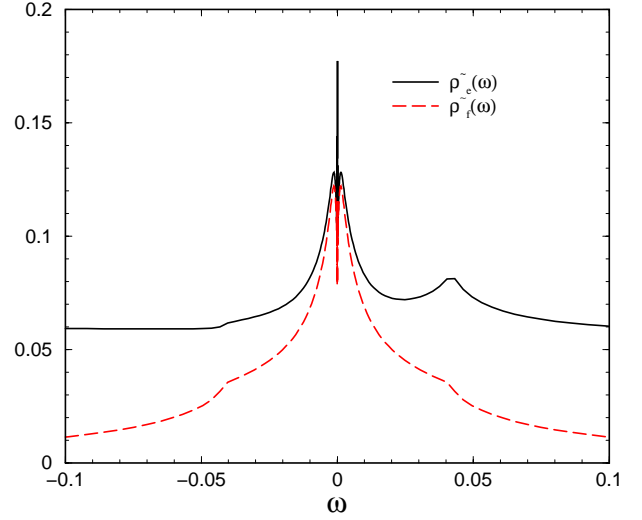

Fig. 8. Quasi-particle media spectral function $\tilde{\rho}_e(\omega) = \Im m\, e(\omega - \mathrm{i}\delta)/\pi$ (solid line) and anomalous media spectral function $\tilde{\rho}_f(\omega) = \Im m\, f(\omega - \mathrm{i}\delta)/\pi$ (dashed line) in DMFT(NCA) in the superconducting phase close to T_c. $\varepsilon_{\alpha\sigma} = -2$.

5.4 One-particle spectra in the triplet-triplet sector

We obtained a self-consistent solution of DMFT(NCA) equations for T close to T_c in the superconducting phase. For $T < T_c$, the ionic propagators [31–33] aquire an additional self-energy contribution which originates from the anomalous conduction-electron bath $\tilde{f}$ and is generated by the second diagram of the generating functional $\Phi_{\mathrm{NCA}}^{\mathrm{SC}}$ depicted in Figure 6. These corrections are self-consistently taken into account in our numerics and modify the quasi-particle t-matrices and generate an anomalous t-matrix as depicted in Figure 7. We start the iteration with a finite anomalous media $\tilde{f}_0(z) = A/(z + \mathrm{i}T)$ where the weight A is of the order of 10^{-3}. The temperature at which a finite anomalous t-matrix T_s is stabilized coincides with the instability of the pair-susceptibility. Above T_c, $\tilde{f}(z)$ and $T_s(z)$ approach zero rather rapidly while iterating equations (67–70).

The spectral functions of the effective quasi-particle and anomalous media is plotted in Figure 8: a delta peak at $\omega = 0$ is growing on top of the regular part similar to the reported media in the single-channel Anderson lattice at $T = 0$, shown in Figure 3 of reference [46]. This delta peak should lead to a Fermi-liquid form of the quasi-particle self-energy Σ_{11} for $T \to 0$. We clearly see the decrease of the quasi-particle scattering rate slightly below T_c as shown in Figure 9. This suppression of the quasi-particle scattering rate indicates the removal of the residual entropy of the normal state: the magnetic scattering is strongly reduced due to forming a composite order parameter entangling local magnetic (quadrupolar) degrees of freedom with spin singlet/quadrupolar triplet Cooper pairs.

The local quasi-particle and anomalous Green function is shown in Figure 10. It develops a pseudo-gap for very low frequencies which behaves like $|\omega|$ as indicated by
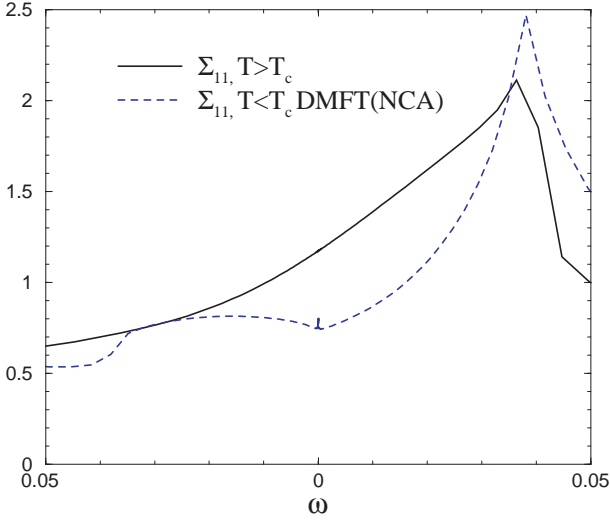
Fig. 9. Comparison of the imaginary part of the quasi-particle self-energy in the normal state, which is also used in approximation (i), close to T_c (solid line) and the self-energy $\Im m \Sigma_{11}(\omega - i\delta)$ obtain through (73) and the full DMFT(NCA) (dashed line). Parameters as in Figure 8.
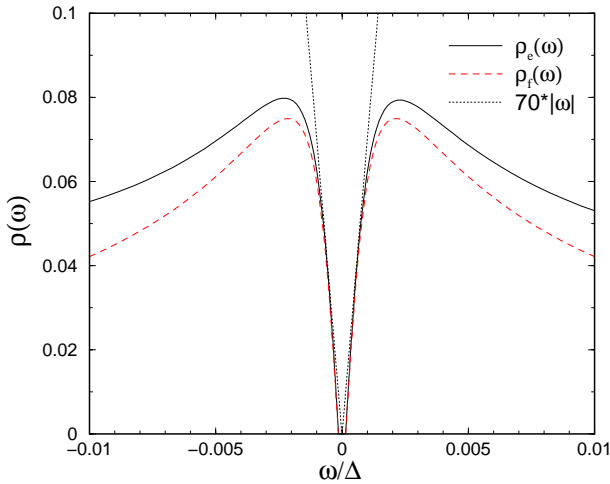

Fig. 10. Spectral functions of the quasi-particle and the anomalous Green function in DMFT(NCA) in the superconducting phase for $1 - T/T_c \ll 1$ in the vicinity of $\omega = 0$. The dotted curve shows a fit with $a * |\omega|$. Parameters as in Figure 8.

the dotted fit curve in Figure 10. This approximate $|\omega|$-dependency of the spectral functions can be understood analytically. It is apparent from the evaluation of equation (66) that the frequency dependency of the spectral function is determined by the imaginary part of the inverse of the determinant $\sqrt{(z - (\Sigma(z) + \Sigma(-z))/2)^2 - g^2(z)}$. Let us assume that the leading contribution to $g(z)$ can be approximated by a temperature-broadened Lorentzian $A^2/(z + i \, \mathrm{sign}(\Im m z) \alpha T)$, which reflects the $1/z$ divergency of $\Pi_f(i\omega_n, i\omega_m; 0)$ at $T = 0$ (see Eq. (21)); the weight A is proportional to the order parameter, and α a dimensionless constant of the order of $O(1)$. Due to this $1/z$ divergency, its analytic behaviour has similarities to the odd

frequency mean-field solution of the anomalous self-energy by Coleman *et al.* [43], who found that $g(z) = \Sigma_{12} \propto 1/z$.

6 Conclusion

There is a controversial debate (see [25] and reference therein) as to whether an odd-frequency solution with a COM momentum $Q = 0$ is connected to a minimum or a maximum of the free energy and, hence, may be thermodynamically unstable. Assuming a Fermi-liquid normal phase and the occurrence of an infinitesimal odd-frequency anomalous self-energy $g(z)$ at T_c, which implies a second order phase transition, Heid showed that one indeed obtains an increase of the free energy in the superconducting phase for $Q = 0$ [25]. We will give two arguments why we believe, in our case on the contrary, that the superconducting phase is thermodynamically stable, even though we cannot prove unambiguously whether the phase transition is first order or continuous. It is straightforward to extend Heid's theorem onto a non-Fermi liquid normal phase. An infinitesimal and analytic odd-frequency $g(z)$ does lead to an enhancement of the quasi-particle DOS ρ at $\omega = 0$ and hence to a maximum in the free energy. However, based on the self-consistent solution for the anomalous Green functions (67–70), $g(z)$ converges to a finite value such that Γ_s is approximately $\Gamma_s \approx \Gamma_{qp}$ generating a gap in the lattice Green functions similar to the one reported earlier [43]. $g(z)$ might be approximated in leading order by a Lorentzian with a finite weight $\tilde{g} \approx \sqrt{\Gamma_{qp} \alpha T}$. The assumption of an infinitesimal value of $g(z)$ for all frequencies is violated and hence Heid's theorem is not applicable in our case. Since the order parameter then has a finite value at the transition, the phase transition would be first order and the associated latent heat $L = T_c(S_N - S_s)$ would be related to the change of entropy. However, in the presence of an anomalous medium, the quasi-particle self-energy is also modified and, therefore, the feedback into the effective site must be calculated self-consistently. The generating functional for the local site in a superconducting medium is shown in Figure 6 for the NCA. We expect that the self-consistent solution for the one-particle Green function in the superconducting phase will show a vanishing scattering rate for the quasi-particle at $\lim_{\omega \to 0} \Gamma_{qp} \to 0$. In this case, a non-analytic $g(z)$, even with an infinitesimal $\tilde{g}$, will be able to always produce a gap.

It turns out, however, that the DMFT(NCA) equations for the superconducting phase are numerically unstable for $T \ll T_c$. We believe that the instability of the equations is related to the known inability of the NCA to reproduce the Fermi-liquid phase of the periodic Anderson model [17,19]. It is clearly related to the occurrence of an additional very sharp delta peak in the media spectra (Fig. 8). Nevertheless, the solutions obtained at T_c show a reduction of the local free energy in the presence of a finite anomalous Green function and a tendency to reduce the scattering rate for the quasi-particles. Therefore, even though we cannot derive conclusively the type of the phase transition, we believe that there are strong hints towards
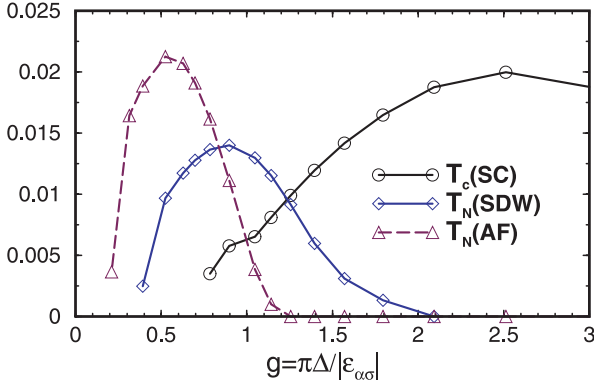
Fig. 11. The phase diagram of the two-channel periodic Anderson model for $n_c = 2.2$: the superconducting transition temperature T_c, the antiferromagnetic transition temperature $T_m(AF)$, the spin-density wave transition temperature $T_m(SDW)$ are plotted *versus* the effective dimensionless coupling constant $g = \pi\Delta/|\varepsilon_{\alpha\sigma}|$. Spin/channel triplet superconductivity dominates the IV regime and the cross-over region to the Kondo regime.

a second order transition in the StCt sector. This phase transition should be associated with a minimum of the free energy since an energy gap develops in the spectrum of the local band Green function indicating an energy gain by condensation.

6.1 Phase diagram and experimental relevance

The phase diagram shown for $n_c = 2.2$ in Figure 11 summarizes our investigation of superconductivity and magnetism in the two-channel Anderson model. Superconductivity dominates the intermediate valence regime and the corresponding order parameter has StCt symmetry. An instability in the SsCs reported in the two-channel Kondo lattice could be reproduced but occurs at much lower temperatures.

The magnetic or quadrupolar phases of the model was discussed in a previous publication [14]: Ferromagnetism is only found for low band fillings $n_c \approx 1$. Spin-density wave phase transitions take over in the Kondo-regime at $g \approx 1.3$ corresponding to $\varepsilon_{\alpha\sigma} = -2.4$. The SDW wave-vector is continuously shifted towards nearest-neighbour antiferromagnetism, which is suppressed for $g \to 0$. Since all calculations were performed in the paramagnetic phase of the model, the highest transition temperature defines the nature of the incipient order. It cannot be ruled out, however, that an SDW phase is replaced by, or even coexists with, a superconducting phase as found in some uranium based Heavy Fermion compounds. Since the quasi-particle spectral function vanished linearly for $\omega \to 0$, $\rho(w) \propto |\omega|$ as depicted in Figure 10, for a spatially isotropic gap function, the specific heat obeys a power law T^α below T_c. Additional anisotropic components $\propto \varepsilon_{\boldsymbol{k}}$ contribute in the intermediate valence regime. Therefore, a exponent $2 < \alpha < 3$ is expected: a value of $\alpha \approx 2.8$ was experimentally observed on UBe_{13}.
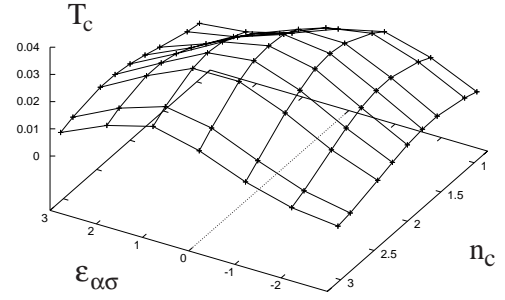

Fig. 12. The transition temperature T_c as function of the level difference $\varepsilon_{\alpha\sigma}$ and the conduction band filling. $n_c = 2$ corresponds to half-filling. Note the inversion of the axis scale in order to visualize more clearly the dependency of T_c for $\varepsilon_{\alpha\sigma} \approx 1$ and for large band fillings n_c, a regime which might be of interest with respect to UBe_{13}.

In the traditional approaches to heavy fermion superconductivity, one solely focuses on possible $\boldsymbol{k}$-dependency of the gap function with nodes on the Fermi surface in order to explain the power-law dependency of the specific heat, for instance. Here, we presented a pairing mechanism which leads to a gap function with nodes in frequency space additionally to a $\boldsymbol{k}$ dependence $\propto \varepsilon_{\boldsymbol{k}}$. The pairing interaction correlates spatially extended, nearest neighbor Cooper-pairs to local spin or quadrupolar moments. It was not necessary to introduce finite center of mass momentum Cooper-pairs, *i.e.* $\boldsymbol{Q} \neq 0$, to observe the phase transition into this state. Finite $\boldsymbol{Q}$ Cooper-pairs would imply a persisting current, and phases of this kind have sofar not been observed experimentally.

Assuming a quadrupolar ground state of the uranium ion, Figure 11 will show the phase diagram for quadrupolar order since spin and channel indices are just exchanged. The superconducting order parameter, however, is not affected by this transformation as discussed in Section 3.3. The tensor order parameter O_{ij}, (44), transforms as $SO(3) \otimes SO(3)$. In a cubic crystalline field environment, this order parameter reduces to $\Gamma_1 \oplus \Gamma_3 \oplus \Gamma_4 \oplus \Gamma_5$ and the phenomenological approach by Sigrist and Rice [47] is still applicable in our case.

Complicated phase diagrams as found in Thorium doped $U_{1-x}Th_xBe_{13}$ are explained by order parameters of different irreducible representation. Recently, the second phase transition of $U_{1-x}Th_xBe_{13}$ was interpreted as a magnetic phase [48] coexisting with the superconducting phase. If our model has any relevance for $U_{1-x}Th_xBe_{13}$, we would expect an antiquadrupolar order or a quadrupolar density wave, since a magnetic ground state of uranium contradicts the weak magnetic response of van-Vleck type [49].

The superconducting transition temperature $T_c(\varepsilon_{\alpha\sigma}, n_c)$, which is shown normalized to T^* in Figure 5, is only symmetric with respect to $\varepsilon_{\alpha\sigma}$ at half filling. We have summarized all the information on $T_c(\varepsilon_{\alpha\sigma}, n_c)/\Delta$ in a 3d-plot displayed in Figure 12. We note that for $\varepsilon_{\alpha\sigma} \approx 1$, *i.e.* an intermediate valence regime with quadrupolar ground state on the local shell as in uranium in cubic environment, T_c decreases with increasing hybridization

and band filling. A similar behaviour is observed in $U_{1-x}Th_xBe_{13}$ where T_c decreases under applied pressure and also under Thorium doping which is interpreted as increasing the number of band-electrons [50].

The skutterudite materials $PrFe_4P_{12}$ and $PrOs_4Sb_{12}$ are also prominent candidates for the $SU(2) \otimes SU(2)$ lattice model, since Pr^{3+} is hosted in a cubic crystalline environment. The anti-quadrupolar ordered ground state is observed in $PrFe_4P_{12}$, while $PrOs_4Sb_{12}$ shows superconductivity below 2K. We expect that $PrFe_4P_{12}$ becomes superconducting under pressure.

Appendix A: Composite order parameter

The composite order parameter can be related to the time derivative of the isotropic and *extended s-wave* anomalous Green functions in the appropriate symmetry sector – see Table 1 in page 14. The analytically continued Matsubara Green function for fermionic operators A and B obeys the equations of motion

$$z\, G_{A,B}(z) = \langle \{A, B\} \rangle - G_{[H,A],B}(z). \tag{75}$$

The commutator of a conduction electron with the local quantum numbers $\alpha\sigma$ at site ν,

$$[H, c_{\nu\alpha\sigma}] = -\psi_{\nu\alpha\sigma} - V_\alpha X^\nu_{-\alpha,\sigma}, \tag{76}$$

is derived from the Hamiltonian (1), where

$$c_{\nu\alpha\sigma} = \frac{1}{\sqrt{N}} \sum_{\boldsymbol{k}} e^{i\boldsymbol{k}\boldsymbol{R}_\nu} c_{\boldsymbol{k}\alpha\sigma} \tag{77}$$

$$\psi_{\nu\alpha\sigma} = \frac{1}{\sqrt{N}} \sum_{\boldsymbol{k}} e^{i\boldsymbol{k}\boldsymbol{R}_\nu} \varepsilon_{\boldsymbol{k}\alpha\sigma} c_{\boldsymbol{k}\alpha\sigma} \tag{78}$$

has been used. Using the equation of motion

$$z\, G_{c_{\nu\alpha\sigma},c_{\nu\alpha'\sigma'}}(z) = G_{\psi_{\nu\alpha\sigma},c_{\nu\alpha'\sigma'}}(z) + V_\alpha G_{X^\nu_{-\alpha,\sigma},c_{\nu\alpha'\sigma'}}(z) \tag{79}$$

to calculate the equal time expectation value of the time derivative $\langle \frac{d}{d\tau} c_{\nu\alpha\sigma}(\tau) c_{\nu\alpha'\sigma'} \rangle$ in the form

$$D^{\alpha\alpha'}_{\sigma\sigma'} = \frac{1}{\beta} \sum_{i\omega_n} e^{i\omega_n\delta} i\omega_n G_{c_{\nu\alpha\sigma},c_{\nu\alpha'\sigma'}}(i\omega_n) \tag{80}$$

yields

$$D^{\alpha\alpha'}_{\sigma\sigma'} = \langle \psi_{\nu\alpha\sigma} c_{\nu\alpha'\sigma'} \rangle + V_\alpha \langle X^\nu_{-\alpha,\sigma} c_{\nu\alpha'\sigma'} \rangle. \tag{81}$$

The first term on the r.h.s. represents the averaged kinetic energy, which is zero in the case of an odd-frequency

anomalous Green function $G_{c_{\boldsymbol{k}\alpha'\sigma'},c_{-\boldsymbol{k}\alpha\sigma}}(z)$, while the second describes the coupling to the localized f-shell. Using the commutator

$$[H, X^\nu_{\alpha,\sigma}] = (E_\alpha - E_\sigma)X^\nu_{\alpha,\sigma} - V_{-\alpha}\sum_{\sigma'} X_{\sigma',\sigma} c_{\nu-\alpha\sigma'}$$
$$- \sum_{\alpha'} V_\alpha X_{\alpha,-\alpha'} c_{\nu\alpha'\sigma}, \tag{82}$$

and

$$C^{\alpha\alpha'}_{\sigma\sigma'} = \frac{1}{\beta} \sum_{i\omega_n} e^{i\omega_n\delta} i\omega_n \left(G_{X^\nu_{\alpha,\sigma},c_{\nu'\alpha'\sigma'}}(i\omega_n) \right.$$
$$\left. + G_{c_{\nu'\alpha'\sigma'},X^\nu_{\alpha,\sigma}}(i\omega_n) \right) \tag{83}$$

we derive

$$2V B^{\alpha\alpha'}_{\sigma\sigma'}(\nu) = C^{\alpha\alpha'}_{\sigma\sigma'} - 2(E_\sigma - E_\alpha) \langle X^\nu_{\alpha,\sigma} c_{\nu'\alpha'\sigma'} \rangle \tag{84}$$

via equation of motion and, therefore, with $\Delta E = E_\sigma - E_\alpha$ and $V_\alpha = \alpha V$

$$|\Delta E| D^{\alpha\alpha'}_{\sigma\sigma'} - \text{sign}(\Delta E)\alpha \frac{V C^{\alpha\alpha'}_{\sigma\sigma'}}{2} =$$
$$-\alpha V^2 \text{sign}(\Delta E) B^{\alpha\alpha'}_{\sigma\sigma'}(\nu). \tag{85}$$

The quantity $B^{-\alpha\alpha'}_{\sigma\sigma'}(\nu)$ is defined as

$$B^{-\alpha\alpha'}_{\sigma\sigma'}(\nu) = \alpha \sum_{\sigma''} \langle X_{\sigma'',\sigma} c_{\nu\alpha\sigma''} c_{\nu'\alpha'\sigma'} \rangle$$
$$+ \sum_{\alpha''} \alpha'' \langle X_{-\alpha,-\alpha''} c_{\nu\alpha''\sigma} c_{\nu'\alpha'\sigma'} \rangle. \tag{86}$$

A relation for $C^{\alpha\alpha'}_{\sigma\sigma'}$ can be derived using (75) and (82)

$$\alpha V C^{-\alpha\alpha'}_{\sigma\sigma'} = -2\frac{1}{\beta} \sum_{i\omega_n} e^{i\omega_n\delta} i\omega_n G_{\psi_{\nu\alpha\sigma},c_{\nu\alpha'\sigma'}}(i\omega_n)$$
$$= -2\tilde{T}^{\alpha\alpha'}_{\sigma\sigma'}, \tag{87}$$

and the assumption that the anomalous Green function is odd in frequency. If only pairs with COM momentum $\boldsymbol{Q} = 0$ condensate, the condition

$$G_{c_{\boldsymbol{k}\alpha'\sigma'},c_{-\boldsymbol{k}'\alpha\sigma}}(z) = \delta_{\boldsymbol{k},\boldsymbol{k}'} G_{c_{\boldsymbol{k}\alpha'\sigma'},c_{-\boldsymbol{k}\alpha\sigma}}(z)$$

holds. Then $\tilde{T}^{\alpha\alpha'}_{\sigma\sigma'}$ is equal to $T^{\alpha\alpha'}_{\sigma\sigma'}$, defined in equation (41). It is straightforward to show that

$$\left(\langle \boldsymbol{S}\, \boldsymbol{P}^{t,s} \rangle - \langle \boldsymbol{\tau}\, \boldsymbol{P}^{s,t} \rangle \right) = -\sum_{\alpha\sigma} \sigma B^{\alpha\alpha}_{\sigma-\sigma} \tag{88}$$

and to obtain the equation (42) from (85) and (88):

$$O_{ss} = \frac{|\Delta E|}{|V|^2} \sum_{\alpha\sigma} \alpha\sigma D^{\alpha-\alpha}_{\sigma-\sigma}$$
$$+ \frac{\text{sign}(\Delta E)}{V^2} \sum_{\alpha\sigma} \alpha\sigma T^{\alpha-\alpha}_{\sigma-\sigma}. \tag{89}$$

Equations (85) and (88) in conjunction also yield equation (44) on page 16 for the order parameters in Section 4.

Appendix B: Calculation of the odd-frequency pair-susceptibility

Assuming we know the irreducible particle-particle vertex $\underline{\underline{\Gamma}}^{pp}_{irr}$ for the appropriate symmetry and only consider isotropic pairs, then the pair-susceptibility of the composite order parameter is proportional to

$$\chi_P(\boldsymbol{q}) =$$
$$\frac{1}{\beta} \sum_{n,n'} \omega_n \omega_{n'} \left[\underline{\underline{\chi}}(\boldsymbol{q}, 0) \frac{1}{\underline{\underline{1}} - \frac{1}{\beta} \underline{\underline{\Gamma}}^{pp}_{irr}(0) \underline{\underline{\chi}}(\boldsymbol{q}, 0)} \right]_{\mathrm{i}\omega_n \mathrm{i} w_{n'}}. \quad (90)$$

Since $\underline{\underline{\chi}}(\boldsymbol{q}, \mathrm{i}\nu_n)$ is diagonal in Matsubara frequency space, $\sqrt{\underline{\underline{\chi}}(\boldsymbol{q}, 0)}$ is a well defined quantity so that a new symmetrical matrix $\underline{M}$

$$\underline{\underline{M}} = \sqrt{\underline{\underline{\chi}}(\boldsymbol{q}, 0)} \frac{1}{\beta} \underline{\underline{\Gamma}}^{pp}_{irr}(0) \sqrt{\underline{\underline{\chi}}(\boldsymbol{q}, 0)}, \quad (91)$$

can be introduced. It is diagonalized to obtain the base $|\lambda\rangle$, equation (48), $\underline{M}|\lambda\rangle = \lambda|\lambda\rangle$ and to rewrite $\chi_P(\boldsymbol{q})$

$$\chi_P(\boldsymbol{q}) = \frac{1}{\beta} \langle \omega_n | \sqrt{\underline{\underline{\chi}}(\boldsymbol{q}, 0)} \left[\underline{\underline{1}} - \underline{\underline{M}} \right]^{-1} \sqrt{\underline{\underline{\chi}}(\boldsymbol{q}, 0)} | w_n \rangle, \quad (92)$$

where $|w_n\rangle = (\cdots, \omega_n, \cdots)^T$. This eigenvalue equation is viewed as the analog to the linearized Eliashberg equation in the standard theory of superconductivity, even though no reference to Migdal's theorem was made here. We can use all eigenvectors $|\lambda\rangle$ as a complete base in frequency space

$$\hat{1} = \sum_\lambda |\lambda\rangle\langle\lambda| \quad (93)$$

and insert it into (92) to obtain

$$\chi_P(\boldsymbol{q}) = \frac{1}{\beta} \sum_\lambda |\underbrace{\langle\lambda| \sqrt{\underline{\underline{\chi}}(\boldsymbol{q}, 0)} |\omega_n\rangle}_{c_\lambda}|^2 \frac{1}{1 - \lambda}. \quad (94)$$

Since $\sqrt{\underline{\underline{\chi}}(\boldsymbol{q}, \mathrm{i}\nu_n)} |\omega_n\rangle$ is an odd-frequency vector, only odd-frequency eigenvectors $|\lambda\rangle$ contribute to $\chi_P(\boldsymbol{q})$. The leading contribution is given by the eigenvector $|\lambda_c\rangle$ for which $|1 - \lambda|$ has a minimum. Hence, we can write

$$\chi_P(\boldsymbol{q}) = \underbrace{\frac{1}{\beta} c_{\lambda_c}^2 \frac{1}{1 - \lambda_c}}_{P_s(\boldsymbol{q})} + \text{regular terms.} \quad (95)$$

It is now obvious that the pair-susceptibility $\chi_P(\boldsymbol{q})$ diverges when $\lambda_c \to 1$, and that $P_s(\boldsymbol{q})$ is positive in the paramagnetic phase.

Appendix C: One-particle self-consistency condition for local cooper pairs

In DMFT, a purely local self-energy leads to a self-consistency condition (SCC), which states that the $\boldsymbol{k}$-summed one-particle lattice Green function equals the Green function calculated for an effective site with excitations into a surrounding effective medium:

$$\underline{\underline{G}}_c(z) = \frac{1}{N} \sum_{\boldsymbol{k}} \left[\left[\underline{\underline{G}}^0_c(\boldsymbol{k}, z) \right]^{-1} - \underline{\underline{\Sigma}}_c(z) \right]^{-1} \quad (96)$$

$$\left[\underline{\underline{\tilde{G}}}_c(z) \right]^{-1} = \left[\underline{\underline{G}}_c(z) \right]^{-1} + \underline{\underline{\Sigma}}_c(z). \quad (97)$$

$\underline{\underline{G}}^0_c(\boldsymbol{k}, z)$ denotes the Green function in the absence of any interaction, and $\underline{\underline{\tilde{G}}}_c(z)$ denotes the medium or dynamical mean field which enters the effective site problem. It is related to the Anderson width matrix by

$$\underline{\underline{\Delta}}(z) = V^2 \underline{\underline{\tilde{\sigma}}}_2 \underline{\underline{\tilde{G}}}_c(z) \underline{\underline{\tilde{\sigma}}}_2 \quad (98)$$

where $\underline{\underline{\tilde{\sigma}}}_2$ is the 8×8 generalization of σ_2 appropriate to the description of the superconducting state with spin and channel degrees of freedom. It was assumed in Section 5.1 that the orientation in spin and channel space is described by the two unitary vectors. Hence, we use a 2×2 matrix formalism for the dynamics. Close to T_c, e.g. for $g(z) \to 0$, equation (65) is approximated by

$$\underline{\underline{G}}_c(z, \boldsymbol{k}) = \frac{1}{(z - \Sigma_e - \varepsilon_{\boldsymbol{k}})(z - \Sigma_h + \varepsilon_{\boldsymbol{k}})} \quad (99)$$
$$\times \begin{pmatrix} z - \Sigma_h + \varepsilon_{\boldsymbol{k}} & g(z) \\ g(z) & z - \Sigma_e - \varepsilon_{\boldsymbol{k}} \end{pmatrix}$$

$$\Sigma_e = \Sigma(z); \quad \Sigma_h = -\Sigma(-z) \quad (100)$$

in linear order in $g(z)$. The subscripts e and h refer to electrons or holes. We immediately recognize, in conjunction with equation (96), that the quasi-particle properties are not renormalized close to T_c. This is typical for a mean-field theory as the DMFT. With the local electron and hole Green functions

$$e(z) = \frac{1}{N} \sum_{\boldsymbol{k}} \frac{1}{z - \Sigma_e - \varepsilon_{\boldsymbol{k}}}, \quad (101)$$

$$h(z) = \frac{1}{N} \sum_{\boldsymbol{k}} \frac{1}{z - \Sigma_h + \varepsilon_{\boldsymbol{k}}} = -e(-z), \quad (102)$$

we obtain the off-diagonal matrix element

$$f(z) = \left[\underline{\underline{G}}_c(z) \right]_{12} = \frac{e(z) + h(z)}{2z - \Sigma_e - \Sigma_h} g(z), \quad (103)$$

which we insert into the SCC condition (97) with the result

$$\frac{\tilde{f}(z)}{\tilde{e}(z)\tilde{h}(z)} = \frac{f(z)}{e(z)h(z)} - g(z), \quad (104)$$

where $\tilde{e} = \left[\underline{\tilde{\underline{G}}}_c(z) \right]_{11}$ corresponds to the electron medium, and $\tilde{h} = \left[\underline{\tilde{\underline{G}}}_c(z) \right]_{22}$ corresponds to the hole medium. $\tilde{f} = \left[\underline{\tilde{\underline{G}}}_c(z) \right]_{12}$ denotes the anomalous medium in the superconducting phase. $g(\mathrm{i}\omega_n)$ is generated by the particle-particle irreducible vertex $\Gamma_c^{pp}(\mathrm{i}\omega_n, \mathrm{i}\omega_m)$

$$g(\mathrm{i}\omega_n) = -\frac{1}{\beta} \sum_{\mathrm{i}\omega_m} \Gamma_c^{pp}(\mathrm{i}\omega_n, \mathrm{i}\omega_m) f(\mathrm{i}\omega_m) \tag{105}$$

which is local in the DMFT. The anomalous Greens function f can be replaced through the SCC (104) yielding the compact vector equation

$$\left[\underline{\underline{1}} + \frac{1}{\beta} \underline{\underline{\Gamma}}_c \underline{\underline{A}} \right] \underline{g} = -\frac{1}{\beta} \underline{\underline{\Gamma}}^{tt} \underline{\underline{A}} \, \underline{\underline{B}}^{-1} \underline{f}, \tag{106}$$

where

$$[\underline{\underline{A}}]_{n,m} = \delta_{n,m} e(\mathrm{i}\omega_n) h(\mathrm{i}\omega_n) \tag{107}$$

and

$$[\underline{\underline{B}}]_{n,m} = \delta_{n,m} \tilde{e}(\mathrm{i}\omega_n) \tilde{h}(\mathrm{i}\omega_n). \tag{108}$$

Here, we introduced the short hand notation

$$\underline{g} = (\cdots, g(\mathrm{i}\omega_n), \cdots)^T. \tag{109}$$

We use the irreducible vertex (58) and note that $\underline{\underline{\chi}}_{loc} = -\underline{\underline{A}}$ to obtain

$$\underline{g} = -\left[\frac{1}{\beta} \underline{\underline{A}}^{-1} \underline{\underline{\Pi}}_{loc} + \underline{\underline{1}} \right] \underline{\underline{B}}^{-1} \underline{\tilde{f}}. \tag{110}$$

It has been discussed in Section 2.2.3 that the local two particle Green function $\underline{\underline{\Pi}}_{loc}$ (22) can be written as

$$\underline{\underline{\Pi}}_{loc} = -\beta \underline{\underline{A}} + \underline{\underline{B}} \, \underline{\underline{T}}_c \, \underline{\underline{B}}, \tag{111}$$

where $\underline{\underline{T}}_c$ is the local two-particle T-matrix cumulant

$$\underline{\underline{T}}_c = V^4 \left(\underline{\underline{\Pi}}_f^{pp} - \beta \underline{\underline{E}} \right), \tag{112}$$

and $\underline{\underline{\Pi}}_f^{pp}$ the local two-particle f-Green function. Hereby, $[\underline{\underline{E}}]_{n,m} = F(\mathrm{i}\omega_n) F(-\mathrm{i}\omega_n) \delta_{n,m}$. Hence, equation (105) reads

$$\underline{g} = -\frac{1}{\beta} \underline{\underline{A}}^{-1} \, \underline{\underline{B}} \, \underline{\underline{T}}_c \underline{\tilde{f}}. \tag{113}$$

With the matrix equation for the vector $\underline{T}_s = (\cdots, T_s(\mathrm{i}\omega_n), \cdots)^T$

$$\underline{T}_s = -V^4 \frac{1}{\beta} \underline{\underline{\Pi}}_f^{pp} \underline{\tilde{f}}, \tag{114}$$

which can be derived *via* equation of motion or functional derivative, and

$$\frac{\tilde{e}}{e} = \frac{1}{1 + \tilde{e} T_e} \qquad \text{and} \qquad \frac{\tilde{h}}{h} = \frac{1}{1 + \tilde{h} T_h}, \tag{115}$$

we obtain

$$g = \frac{1}{(1 + \tilde{e} T_e)(1 + \tilde{h} T_h)} \left(T_s - T_e T_h \tilde{f} \right) \tag{116}$$

for each frequency $\mathrm{i}\omega_n$ which is just the off-diagonal matrix element of the 2×2 self-energy matrix $\underline{\underline{\Sigma}}$

$$\underline{\underline{\Sigma}} = \underline{\underline{T}} \left[\underline{\underline{1}} + \underline{\underline{\tilde{G}}} \underline{\underline{T}} \right]^{-1} \tag{117}$$

in the limit $f, \tilde{f} \to 0$ where the one-particle T-matrix is given by

$$\underline{\underline{T}} = \begin{pmatrix} T_e & T_s \\ T_s & T_h \end{pmatrix}. \tag{118}$$

In equations (115–118), the energy argument $\mathrm{i}\omega_n$ was dropped for simplicity. In general, $\underline{\underline{\Sigma}}$ reads

$$\underline{\underline{\Sigma}} = \frac{1}{A} \begin{pmatrix} T_e + \tilde{h}(T_e T_h - T_s^2) & T_s - \tilde{f}(T_e T_h - T_s^2) \\ T_s - \tilde{f}(T_e T_h - T_s^2) & T_h + \tilde{e}(T_e T_h - T_s^2) \end{pmatrix} \tag{119}$$

$$A = (1 + \tilde{e} T_e + \tilde{f} T_s)(1 + \tilde{h} T_h + \tilde{f} T_s)$$
$$- (\tilde{e} T_s + \tilde{f} T_h)(\tilde{h} T_s + \tilde{f} T_e). \tag{120}$$

As mentioned above, $g(\boldsymbol{q}, \mathrm{i}\omega_n)$ is generated by the particle-particle irreducible vertex $\Gamma_c^{pp}(\mathrm{i}\omega_n, i\omega_{n'})$, equation (105)

$$g(\boldsymbol{q}, \mathrm{i}\omega_n) = -\frac{1}{N\beta} \sum_{\boldsymbol{k}, \mathrm{i}w_{n'}} \Gamma_c^{pp}(\mathrm{i}\omega_n, \mathrm{i}w_{n'}) f_{\boldsymbol{k}, \boldsymbol{q}}(\mathrm{i}w_{n'}) \tag{121}$$

which is local in the DMFT. On the other hand, we can expand the $\boldsymbol{k}$-dependent anomalous Green's function $f_{\boldsymbol{k}, \boldsymbol{q}}(\mathrm{i}\omega_n)$ close to T_c up to linear order

$$f_{\boldsymbol{k}, \boldsymbol{q}}(\mathrm{i}\omega_n) = -G_{\boldsymbol{k}+\boldsymbol{q}}(\mathrm{i}\omega_n) G_{-\boldsymbol{k}}(-\mathrm{i}\omega_n) \, g(\boldsymbol{q}, \mathrm{i}\omega_n) + O(g^2) \tag{122}$$

in the anomalous self-energy $g(\boldsymbol{q}, \mathrm{i}\omega_n)$ for Cooper pairs with a center of mass momentum $\boldsymbol{q}$. Inserting (122) into (121) and identifying

$$\chi_0^{pp}(\mathrm{i}w_n; \mathrm{i}\nu_n, \boldsymbol{q}) = \frac{1}{N} \sum_{\boldsymbol{k}} G_{\boldsymbol{k}+\boldsymbol{q}}(\mathrm{i}\omega_n + \mathrm{i}\nu_n) G_{-\boldsymbol{k}}(-\mathrm{i}\omega_n) \tag{123}$$

yields

$$g(\boldsymbol{q}, \mathrm{i}\omega_n) = \frac{1}{\beta} \sum_{\mathrm{i}\omega_m} \Gamma_c^{pp}(\mathrm{i}\omega_n, \mathrm{i}\omega_m) \chi_0^{pp}(\boldsymbol{q}, 0) g(\boldsymbol{q}, \mathrm{i}\omega_m). \tag{124}$$

If we set $\underline{g} \propto |\text{eliash}\rangle = \left(\underline{\underline{\chi}}(\boldsymbol{q} = 0, 0) \right)^{-\frac{1}{2}} |\lambda = 1\rangle$, where $|\lambda\rangle$ was a solution of the eigenvalue equation (48) $\underline{\underline{M}}|\lambda\rangle = \lambda|\lambda\rangle$, the vector $|\text{eliash}\rangle$ is a solution of the linearized Eliashberg equation (72). Since $|\lambda = 1\rangle$ corresponds to a diverging pair-susceptibility χ_P (50), a singularity in χ_P is equivalent to a solution of the SCC (97) close to T_c with non-vanishing off-diagonal matrix elements.

References

1. P. Woelfe, D. Vollhardt, *The Superfluied Phases of Helium 3* (Taylor and Francis, London, 1990), for a book on ^{3}He
2. J. Bardeen, L.N. Cooper, J.R. Schrieffer, Phys. Rev. **108**, 1175 (1957)
3. G.M. Eliashberg, Sov. Phys. JETP **11**, 696 (1960)
4. J.W. Allan, B. Mitrovic, Solid State Phys. **37**, 1 (1982), or a review on Eliashberg theory
5. N. Grewe, F. Steglich, in *Handbook on the Physics and Chemistry of Rare Earths*, edited by J.K.A. Gschneidner and L. Eyring (North-Holland, Amsterdam, 1991), Vol. 14, p. 343, for a review on heavy fermions
6. F. Steglich *et al.*, Phys. Rev. Lett. **43**, 1892 (1979)
7. Y. Maeno *et al.*, Nature **372**, 532 (1994)
8. T.M. Rice, M. Sigrist, J. Phys. Cond. Matt. **7**, L643 (1995)
9. G. Baskaran, Physica B **223-224**, 490 (1996)
10. M. Jourdan, M. Huth, H. Adrian, Nature **398**, 47 (1999)
11. for a review of the basic ideas see Grewe and Steglich [5]. The literature of the last decade can be classified by these two rather crude categories (unpublished)
12. F.B. Anders, M. Jarrell, D. Cox, Phys. Rev. Lett. **78**, 2000 (1997)
13. M. Jarrell, H. Pang, D.L. Cox, Phys. Rev. Lett. **78**, 1996 (1997)
14. F.B. Anders, Phys. Rev. Lett. **83**, 4638 (1999)
15. D.L. Cox, Phys. Rev. Lett. **59**, 1240 (1987)
16. N. Grewe, Z. Phys. B **67**, 323 (1987)
17. C.I. Kim, Y. Kuramoto, T. Kasuya, Solid State Commun. **62**, 627 (1987)
18. W. Metzner, D. Vollhardt, Phys. Rev. Lett. **62**, 324 (1989)
19. C.I. Kim, Y. Kuramoto, T. Kasuya, J. Phys. Soc. Jpn **59**, 2414 (1990)
20. M. Jarrell, Phys. Rev. B **51**, 7429 (1995)
21. T. Pruschke, M. Jarrell, J.K. Freericks, Adv. Phys. **42**, 187 (1995)
22. A. Georges, G. Kotliar, W. Krauth, M.J. Rozenberg, Rev. Mod. Phys. **68**, 13 (1996), for a review on the DMFT, see also [21]
23. V.L. Berezinskii, JETP Lett. **20**, 287 (1974)
24. E. Müller-Hartmann, Z. Phys. B. **76**, 211 (1989)
25. R. Heid, Z. Phys. B **99**, 15 (1995)
26. K.R. Lea, M.J.M. Leask, W.P. Wolf, J. Phys. Chem. Solids **23**, 1381 (1962)
27. D.L. Cox, A. Zawadowski, Adv. Phys. **47**, 599 (1998), for a review on the multi-channel models
28. E.D. Bauer et al., Phys. Rev. B **65**, 100506(R) (2002)
29. J. Hubbard, Phys. Roy. Soc. A **281**, 401 (1964)
30. Y. Kuramoto, in *Theory of Heavy Fermions and Valence Fluctuations*, edited by T. Kasuya, T. Saso (Springer Verlag, Berlin, 1985), p. 152
31. N. Grewe, Z. Phys. B **52**, 193 (1983)
32. Y. Kuramoto, Z. Phys. B **53**, 37 (1983)
33. N.E. Bickers, Rev. Mod. Phys. **59**, 845 (1987)
34. H.B. Pang, D.L. Cox, Phys. Rev. B **44**, 9454 (1991)
35. V.J. Emery, S. Kivelson, Phys. Rev. B **46**, 10812 (1992)
36. F. Bommeli *et al.*, Phys. Rev. B **56**, R10001 (1997)
37. U. Brand, C. Mielsch, Z. Phys. B **75**, 365 (1989)
38. V. Zlatic, B. Horvatic, Solid State Commun. **75**, 263 (1990)
39. T. Obermeier, T. Pruschke, J. Keller, Phys. Rev. B **56**, R8479 (1997)
40. N. Grewe, Z. Phys. B **67**, 323 (1987)
41. E. Müller-Hartmann, Z. Phys. B **57**, 281 (1984)
42. A.V. Balatsky, E. Abrahams, Phys. Rev. B **45**, 13125 (1993)
43. P. Coleman, E. Miranda, A. Tsvelik, Phys. Rev. B **49**, 8955 (1994)
44. E. Abrahams, A.V. Balatsky, D.J. Scalapino, J. R.Schrieffer, Phys. Rev. B **52**, 1271 (1995)
45. V. Martisovits, G. Zarand, D.L. Cox, Phys. Rev. Lett. **84**, 5872 (2000)
46. T. Pruschke, R. Bulla, M. Jarrell, Phys. Rev. B **61**, 12799 (2000)
47. M. Sigrist, M. Rice, Phys. Rev. B **39**, 2200 (1989)
48. F. Kromer *et al.*, Phys. Rev. B **62**, 12477 (2000)
49. M. McElfresh *et al.*, Phys. Rev. B **48**, 10395 (1993)
50. F. Steglich, private communication (unpublished)